The Maricunga Belt (chilean Precordillera) and its hydrothermal alteration zones as revealed by multispectral remote sensing and field studies

Torsten Prinz[1] & Lutz Bischoff [2]

Keywords: Chile, geology, mineral alterations, exploration, remote sensing, Landsat TM, ASTER

Abstract

Remote sensing techniques offer a unique chance to analyse and map wide or nearly inaccessable areas under certain geoscientific aspects in relatively short time and at low cost. Therefore geological field campaigns together with multispectral image analysis were carried out for the Maricunga Belt in the chilenean Precordillera, south of the regional mining settlements San Salvador and Potrerillos (Atacama). On the basis of Landsat-TM 5, ASTER, radar-based DGM-data and field mapping/sampling the lithological/structural characteristics of several OH-bearing hydrothermal alteration zones of mostly Neogene age have been investigated because of their high value for future exploration. The often unknown regional tectonic framework which seems to have controlled the alteration dimensions are also discussed. In order to obtain reasonable lithological classification criteria for the remote sensing data fundamental statistical selection rules like the optimum index factor (OIF) were applied to the combination of single TM bands. Furthermore specific band ratios (5/7; 5/4, 5/1) and principal components were utilized to enhance the spectral properties of the argillized, bleached clay- and/or silica-rich alteration surfaces. Additional spectral measurements were carried out for each representative lithological unit of the alteration zones to estimate the quality of the calculated classifications/ratios for geological mapping. In some cases complementary geochemical data has been studied in order to obtain direct clues for understanding the type of some detected hydrothermal alterations. Finally the achieved data was compiled in a geological map which shows more than 20 hydrothermally altered surfaces in relation to the regional geology and the specific tectonic framework. The influence of three major fault systems (the N-S orientated West Fissure System, the NE-SW orientated Inca De Oro System and a poorly described NW-SE System) for the setting of the alterations seems to be obvious.

1 Introduction

The investigation area is situated in the northern Precordillera of the Chilean Andes, approx. 120 km NE of Copiapó/Atacama. It extends to the Quebrada San Andres/Codocedo in the south (26°55' S), the Cerro Agua Amarga/Quebrada Macobi to the west (69°30' W), Potrerillos/El Hueso to the north (26°30' S) and the Cerros Bravos (69°15' W) to the east (Fig. 1). The highest peak of this part of the Precordillera is the volcano Cerro Bravo Alto with 5313 m above sea level (a.s.l.); the lowest point represents the Quebrada Codocedo with 3000 m a.s.l.. The dividing range of the Cordillera Domeyko (incl. Co. Calderon, Portal El Salitre; Cerros Bravos and Portal Codocedo) is forming the main watershed between the Salar de Maricunga in the Preandine Depression and the Rio Copiapo Valley in the coastal zone. The whole area is economically dominated by mining industries like the open pits of San Salvador (Au, Cu), El Hueso (Au) in the north and the mine Can Can/La Coipa (Au, Ag) in the southeast. Beside these large enterprises a lot of smaller

(1,2 Geol.-Institute., Correnssstr. 24, University of Muenster, D-48149 Muenster, Germany, prinz@uni-muenster.de)

mines or pits do exist but most of them have been abandoned. Apart from the permanent settlements of San Salvador and Portrerillos no regular infrastructure has

developed so most investigation test sites are only hard to access. The climate is semi-desert-like with sporadic precipitation during the short winter. Therefore the vegetation is only sparsely developed and bound to erosional gullies and alluvial filled Quebradas. Due to these circumstances multispectral remote sensing techniques represent a useful tool for the extrapolation of achieved geological field results. The general aim of this study is

- to detect hydrothermally altered rocks in the Maricunga belt by applying multispectral remote sensing techniques
- to determine the dimension of alterations
- to calculated alteration-sensible remote sensing classifications (overlays)
- check its reliability in relation to known prospects
- to correlate their lithological type with field study results (test areas)
- to clarify the influence of different local fracture and regional fault systems for the formation of the altered and partly mineralized zones.

In order to support this study geological mapping, structural analysis and sampling of selected test areas were carried out. The samples were studied in thin sections and by X-ray-diffractometry as well as by spectral measurements in the laboratory.

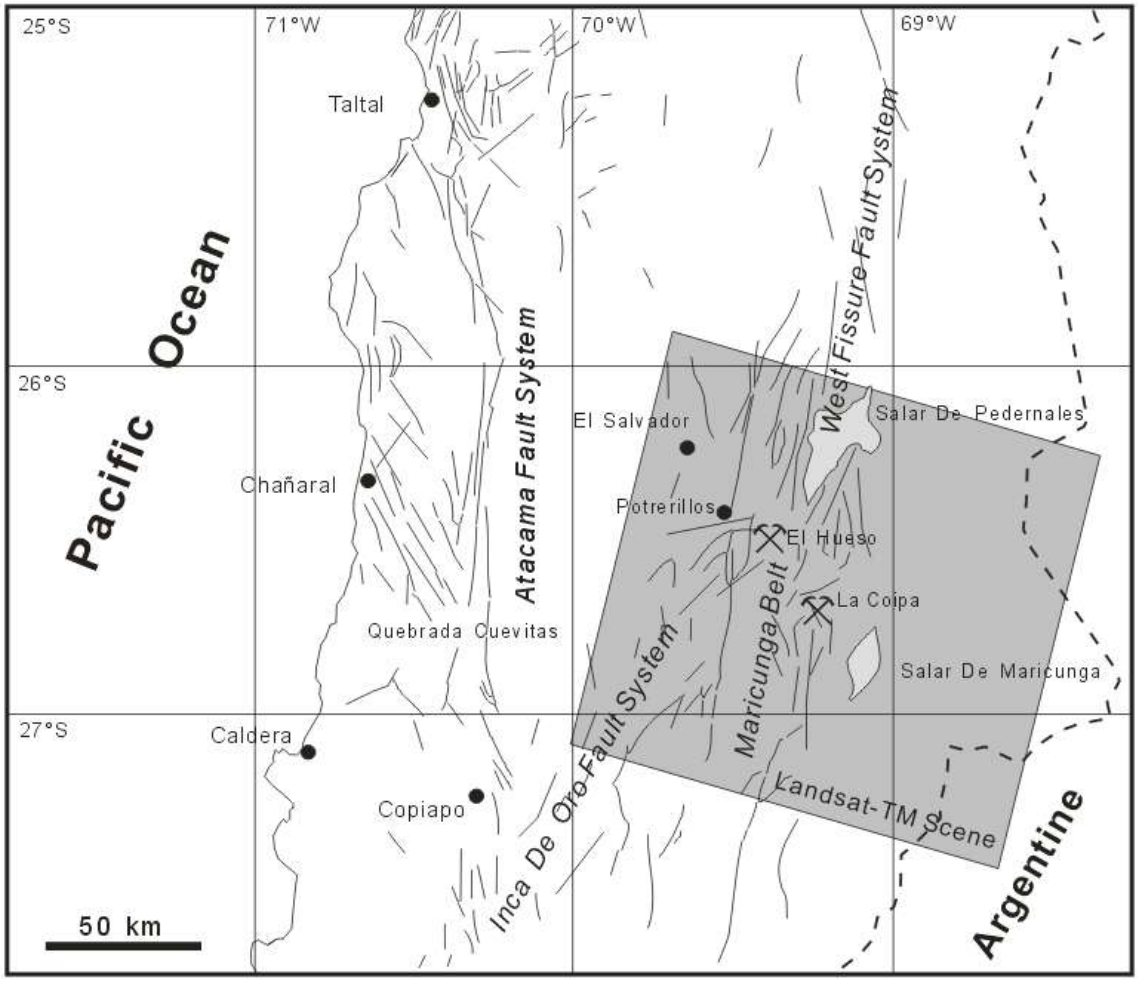

Fig. 1: Shematic location map of the investigation area in northern Chile and the approximate Landsat TM / ASTER data coverage within the Maricunga Belt of the Andes

2 General geological and tectonical setting of Central Northern Andes

The Sierra de Maricunga (Franja de Maricunga) and the Sierra Domeyko represent the Chilean Precordillera which is bordered to the east by the Preandine Depression with the Salar de Maricunga and the Salar de Pedernales. In contrast to more southernly situated segments the Central Chilean Long Valley is missing in this region, so that the Precordillera passes continously into the Coastal Cordillera.
The Andean Orogen generally developed on a basement of Precambrian and Paleozoic rocks. These metamorphic and folded rocks of several orogenic cycles are widespread in the Coastal Cordillera whereas Triassic to Cenozoic rocks of the Andine cycle dominate the Precordillera and the eastern parts of the Central Andes. The geological evolution of the Precordillera of Copiapó, as the whole Anden segment, is controlled by subduction processes at the Nazca / South-America plate boundary. The special situation of the investigated segment results from its transitional position (Cross & Pilger, 1982) between a northern segment between 15° S to 28° S with recent subduction angles about 33° and a southern segment between 28° S and 33° S with a subhorizontal underplating (< 10°). During the Andean evolution a large volume of the Pre-Jurassic continental border was eroded by subduction (Kley et al., 1991; Scheuber, 1994), while the subduction angle, the speed and the angle of convergence changed. In consequence the magmatic arc shifted eastwards in 4 phases beginning in Jurassic times along the Coastal Cordillera, reaching its recent position in the High Cordillera (Davidson & Mpodozis, 1991; Scheuber et al., 1994). Consequently the Precordillera was situated in a marine back arc position from Albian to Cenomanian (110 - 80 m.a.) and was lateron covered by the magmatic arc deposits during Turonian to Oligocene (80 -30 m.a.). In the Sierra de Maricunga magmatic activities were culminating, beginning in the Oligocene (26 m.a.) and lasting to 5 m.a.. During the latter episode of magmatic events most of the surface rocks of the investigation area were formed. Mpodozis et al. (1995) proved with their detailed investigations that five magmatic-tectonic episodes reflect changes in the tectonical framework, the thickening and elevation of the crust and different magma-forming conditions.
The Triassic to Quaternary rocks of the southern segment of the Central Andes underwent mainly brittle deformation of an upper crustal floor. Together with thrust faults open folds occur. Several regional fault systems, mostly strike slip faults, can be distinguished. One of them is the Atacama Fault System (AFS) , which runs N-S over more than 1000 km along the eastside of the Coastal Cordillera, probably initiated in the Jurassic (Scheuber & Andriessen, 1990) with sinistral strike slip movements. However, Pinchera et al. (1990) date its origin in Upper Cretaceous times during an extensive tectonic regime. The history of the movements along the AFS is very complex, but for the last 55 m.a. a dextral-transpressive regime seems to be dominating (Cornejo et al, 1993).
Approximately 80 km further to the east within the Precordillera, the Precordillera Fault System (PFS, also know as the West Fissure System = WFS) developed more or less subparallel to the AFS, showing mainly dextral movements during the Paleogene (Reutter & Scheuber, 1988). Between both N-S- striking systems a broad belt of NW-SE trending faults , the Inca de Oro- Fault System (IFS) has developed under a dextral transpressive regime (Sylvester & Palacios 1992) during Paleocene to Miocene.

2.1 Geology of the investigated area

The investigation area (see also Fig. 21) exhibits outcrops of Permian to Cenozoic rock sequences. The oldest magmatites are Permo-Triassic granites which occur east of the Cerro Vicunita and west of the Quebrada Cienaga. K/Ar dating of biotites

indicate an age of 253 m.a. +/- 8 m.a. (McBride et al., 1976). In some places this granite has an aplitic character, for instance in the smaller outcrops around Caballo Muerte where it has been described in detail by Sindern (1993). Geochemical analysis (Griem, 1994) led to the conclusion that the magmatite evolved in the Paleozoic volcanic arc although some data show a slight affinity towards intraplate granites. This granite is overlain by the Triassic sediments of the La Tenera Formation (sand- and claystones, conglomerates) which crop out around the La Coipa mining district. Fossilized plants indicate a stratigraphic age of Upper Triassic to Pre-Toarcian (Aguilar, 1984). In the mapped area this sequence is developed in form of siltstones with interbedded layers of anthracite. Following Suarez et al. (1994) its sedimentation started in a lacustrine-fluviatile environment and ended in a deltaic fan.
Mesozoic rocks are mainly exposed in the northern and southwestern parts of the Maricunga Belt. The Lower Jurassic formations Asientos and Montadon consist of carbonates, sandstones and basaltic volcanics of Pliensbachian to Callovian age. Griem (1994) emphasizes the 'within-plate' to 'volcanic arc' character of the basalts which dominate the Formation Asientos in the northern and northwestern region.
The continuing deposition of sandy material with carbonatic compounds, often interupted by basaltic outflows, defines the Cretaceous Pedernales Formation (mainly carbonates and volcanics) and the younger Agua Helada/Qda. Monardes Formation (iron-stained red sandstones). Both formations can be found nearly all over the studied area and display a successive shallowing marine sedimentation which proceeds into a final terrestrial, aeolian dune sedimentation on the marginal volcanic back arc. By the end of the Cretaceous time the volcanic-dominated Qda. Paipote/Qda. Seca Formations developed as a result of the progression of the volcanic arc eastwards and a stronger terrestrial influence. The polymict, coarse conglomerates and the unsorted sandstones give record of an extensive alluvial fan with braided river systems within a volcanic source region of intermediate andesites and basalts. Latter rocks crop out near the Vega de Cerros Bravos and northwest of the Qda. Codocedo.

The following Cenozoic terrestrial magmatic rocks are of great importance for the investigation area because of their triggering effect for most of the detected hydrothermal alterations: In the vicinity of Co. Tamberia/Co. El Gallo several outcrops of Paleocene pyroclastics and intrusives of mainly rhyodacitic character can be found. During the Eocene the production of dacitic to rhyolitic volcanics continued, forming the El Hueso, Sierra San Emilio and Co. Valiente volcanic complexes including subvolcanic intrusions and related important zones of hydrothermal alteration (El Hueso!). The dacitic domes of the Vega de Indagua alteration zones are of Middle to Upper Eocene and (together with the smaller Oligocene to Miocene intrusives of the El Hueso area) restricted to the northern parts of the Maricunga Belt.
Neogene Volcanics of the Cerro Bravo/La Coipa complex (mainly ignimbrites or dacites) and the San Andres/Gravas de Atacama formation (ignimbrites and coarse clastites) show isotopic ages of 25.1 (+/- 0.8) m.y. to 20.4 (+/- 1.1) m.y. (Skarmeta, 1985; Mpodozis et al., 1995), which indicates a Lower Miocene formation. These two volcanic units are exposed along the eastern margin of the Maricunga Belt where they enclose the younger, important hydrothermal alteration zones of La Coipa, Pompeya or Vicuñita. The oldest volcanics of this sequence are the latites, ignimbrites and dacites of the La Coipa/Pedregoso/Pompeya region, followed by the younger dacites of Can Can and Paloma. Hellebrandt (1993) estimates a local thickness of the pyroclastics around Co. La Coipa/Co. Bravo of more than 400 m. The youngest rocks of the investigation area are the polymict Quarternary alluvial deposits, accumulated in the main Quebradas.

2.2 Tectonic of the investigated area

The Precordilleran segment between 26° and 27° S is dissected by numerous faults among which the most important structural features are: the Potrerillos Fold and Thrust Belt, the Castillo Fault, the Agua Amarga Thrust Fault, a set of NNW-SSE striking subvertical faults and at their southern ends reverse faults (Fig. 2). All of these fault systems are more or less kinematically related and part of the same deformation during the Upper Eocene Incaic orogenic phase (Cornejo et al. 1993, Abels & Bischoff, 1996).

The Potrerillos Fold and Thrust Belt (PFTB) consists of a multiple set of east verging ramp-flat-style thrusts and folds characterizing a zone of thin skinned tectonics (Olson 1989).The Sierra Castillo normal Fault limits the PFTB on ist western side, strikes NNE-SSE and dips steeply to the east or is subvertical (Cornejo et al. 1993). South of a small cross element with complex structures near Potrerillos and the mine El Hueso the thrusts of the PFTB change their strike into N-S and further south some of them turn into the set of NNW-SSE faults. The Sierra Castillo Fault seems to continue southward over the cross element of Potrerillos into the Agua Amarga Fault Zone. However this southern part of the Precordillera Fault System has a quite different character with obvious thrusting towards the east. The Agua Amarga Reverse Fault forms the western limit of the domaine of the set of long NNW-SSE strike slip faults with sinistral displacements of up to 3,5 - 4 km. The evolution of these main fault systems in this part of the Precordillera can be seen as a response of an old deep-seated crustal sutur to the increase of compression during the Upper Eocene Incaic phase caused by the strong northeast to eastnortheast directed subduction of oceanic crust under the South American continent at that time (Abels & Bischoff, 1996). The position of the old suture line becomes apparent by a number of structural anomalies which extend from Taltal on to Potrerillos and the Valle Ancho. Mpodozis et al. (1995) interpret this line as the northern boundary of the Chilenia terrane which has been accreted to Gondwana in Devonian times. The reactivation of the paleo-suture could have led to sinistral shear movements along the already existing NNW-SSE faults which now acted as oblique ramps between two large crustal blocks during their clockwise rotation (Abels & Bischoff, 1996).

The fault systems described above are of an regional importace, but in some areas smaller sstructures, like NE-SW striking faults play also an important role for the mineralization of precious ore mining prospects (Vila & Silitoe, 1991; Moscoso et al., 1992; Mpodozis et al., 1995; Sindern et al., 1996).

2.3 Hydrothermal Alterations

In many places rocks of the investigated area underwent a hydrothermal alteration of meso- to epithermal character during the volcanotectonic activities. Related to these mineralizations different ore deposits, especially hydrothermally triggered Au-, Ag- and Cu- enrichments developed which are of a high economic interest today. The gold-silver deposits of the Maricunga Belt are some of the biggest epithermal

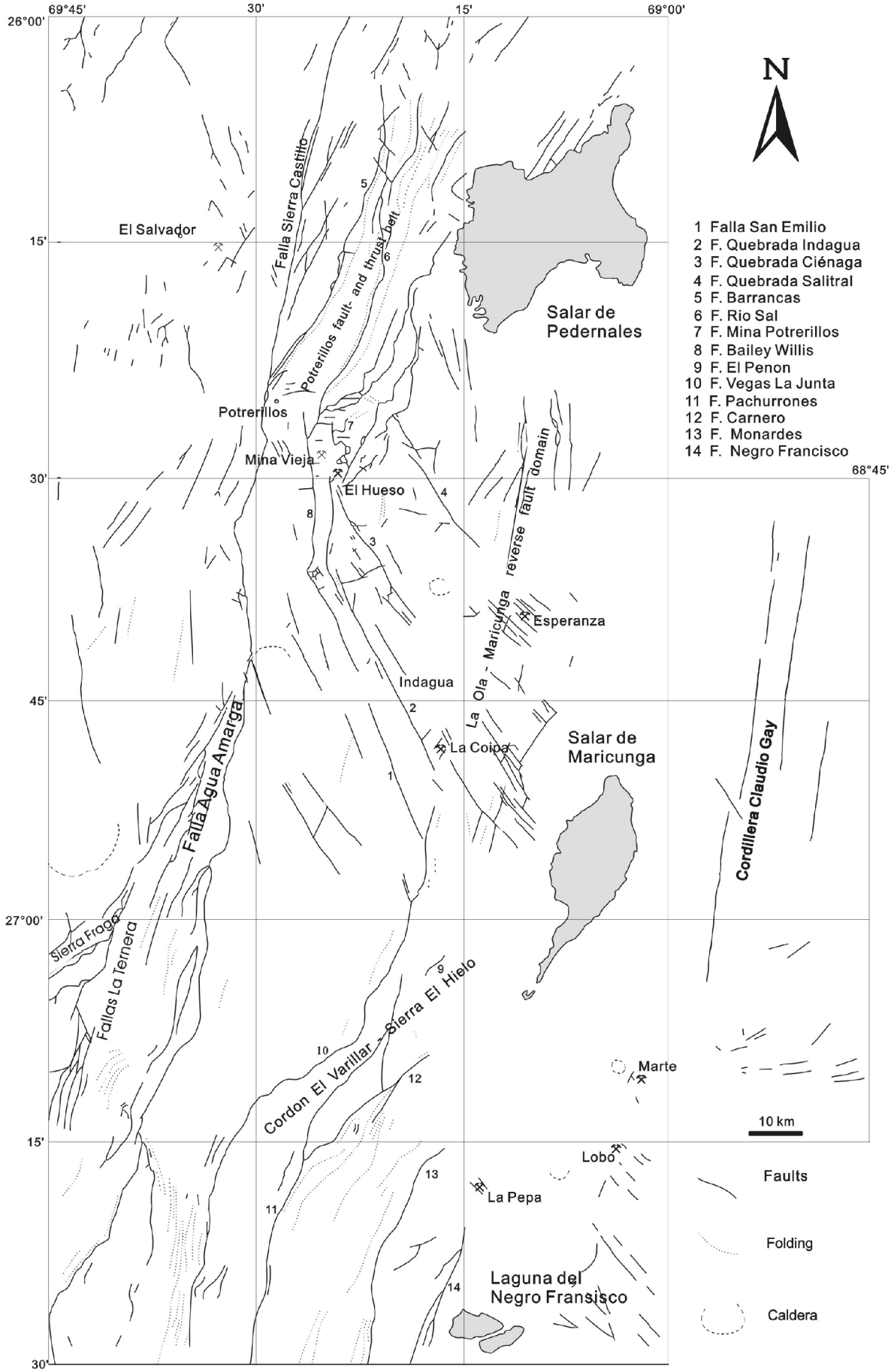

Fig. 2: Simplified map of the major tectonical fault systems of the Maricunga Belt, compiled after field and remote sensing studies (partly modified after ABELS, 1995).

precious metal concentrations in Chile. The origin of the deposits is spatially and temporally related to Cenozoic volcanism and its associated low sulfur (adular sericite paragenesis) and high sulfur (alunite-kaolinite paragenesis) type of alteration. The latter type is characterized by alunite, kaolinite, a high amount of different clay minerals (argillic alteration), chlorite and accessoric sericite. Especially alunite, kaolinite and clay minerals are of high indicative value for the detection of future prospects by multispectral remote sensing techniques, due to their strong OH-absorption features in the infrared (IR). But even in the visual spectra (VIS) these special zones are easy to detect in the field by the abnormal brightness of their bleached surfaces (Fig. 3) due to the high albedo of clayminerals and often occuring adittional silifications, forming so called 'vuggy silicas' (due to the weathering and erosional decay of secondary clay minerals, creating some mm to cm large box-holes in the silicified rock [STOFFREGEN, 1987]).

Fig. 3: Hydrothermally altered and argillized Neogene pyroclastics southwest of Can Can (test site II), showing a high albedo in the visible spectra.

The extension of the alterations are mainly restricted by the mobility of the circulating mineral enriched waters within the country rock, which is controlled by structural elements (e.g. faults) and the lithological properties (e.g. permeability). According to the field data SINDERN et al. (1995) emphazises that especially the pyroclastics are affected by different type of hydrothermal pressure, leading to different alterations/Au-mineralizations supported by their high permeability and their immediate vicinity to the responsible epithermal sources (Fig. 4). The most important alteration zones of the investigation area are from north to south (see appendix map): El Hueso, Cerro Silica, Agua Armarga, Vega del Valiente, Cerro Colorado, Cerro Indagua, Cerro Vicuñita, Pompeya, Can Can and La Coipa (Ladera, Farellon).
In the following a special focus is set on the Cerro Indagua volcanic complex and the La Coipa volcanic complex in order to determine the reliability of multispectral image enhancing techniques for the detection and discrimination of hydrothermally altered rocks in areas which have been mapped in detail with conventional methods.

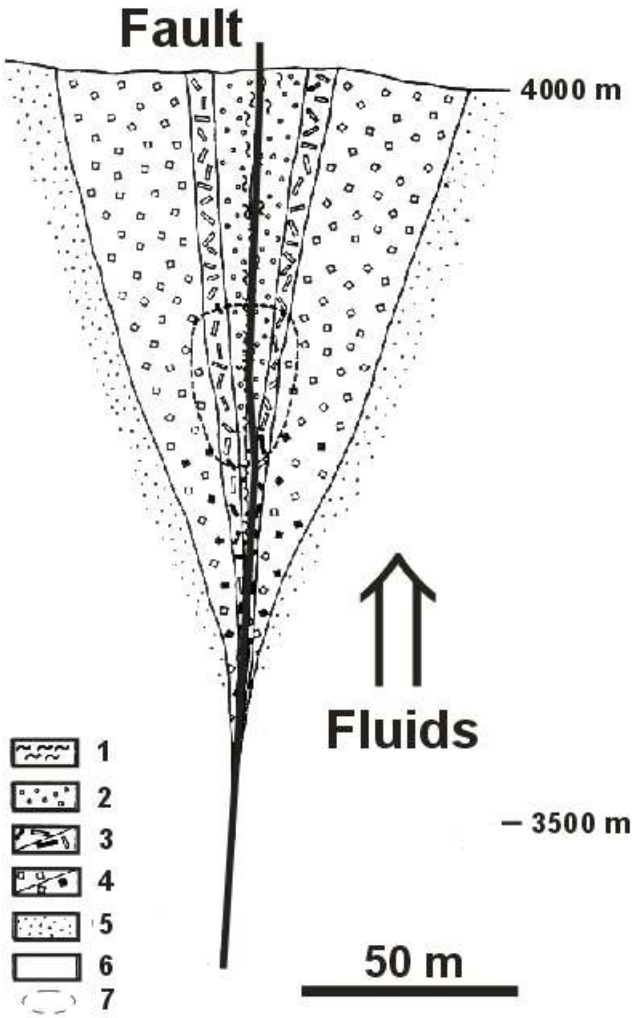

Fig. 4: Generalized hydrothermal alteration zoning along common fault structures of the Maricunga Belt (1 = hydrothermal breccia; 2 = vuggy silica (quartz); 3 = intensive clay mineral alterations (alunite, kaolinite and quartz); 4 = moderate clay mineral alterations (kaolinite and quartz); 5 = marginal clay mineral alterations (montmorillonite and sepiolite); 6 = non altered country rock; 7 = potentially Au- and Ag-enriched alteration zones, modified after SINDERN et al., 1995).

4 Remote sensing methodology

In order to link the spectral properties of the surface material in some test areas with calculated optimized TM colour composites this study adopted three different methods: The first one is based on the laboratory spectral measurements of representative rock samples from different alteration zones and the definition of detectable lithological classes using ground truth. The second one is the statistical analysis of all digital numbers (DN) within the reflective TM bands of the subscene and the determination of suitable colour composites based on the statistical parameter of each component. This step includes maximum likelihood classifications of predefined alteration classes based on enhanced band ratios (e.g. OH-bearing argillized minerals, Fe- and silica-rich surfaces). In the third step the best fit classification results are checked for their possible reliability to field and tectonical observations in this region. In addition multispectral ASTER-data (Advanced Spaceborn Thermal Emission and Reflexion Radiometer, which show a higher geometrical resolution then TM data) where combined with radar-generated altimetric data (SRTM-type) to provide virtual impressions of the altered locations and their morpho-tectonic shape.

4.1 Spectral measurements

During the geological field campaigns of 1989 - 1997 several representative rock samples were taken from exposed stratigraphic units out of each test site/alteration area. Due to the extreme desert-like climate of the Atacama the vegetation was only sparsely developed and confined to some seasonal gullies and 'Quebradas' like the Qda. Indagua. Therefore soils, sand, alluvial deposits, hydrothermal altered surfaces and outcropping geological formations are well exposed and readily detectable by the TM- and ASTER-scanner. In consequence the spectral properties of the material were relatively unmasked, except of the existence of desert varnish on rock surfaces in some places (later measurements showed that this varnish caused a decrease of the reflectance intensity around 15 to 20%, while the important absorption features were still expressed!). Altogether the spectral properties of more then 60 samples (including loose sand and pulverized coarse alluvium) were measured over the continuous wavelenght region from 400 to 2500 nm in relation to the TM scanner sensibility range, applying a Lamnda-9 photospectrometer of the Bundesanstalt fuer Geowissenschaften und Rohstoffe (BGR) in Hannover/Germany (PERKIN-ELMER, 1993).

Due to the fact that most rocks of the Maricunga Belt are andesites, diorites, (rhyo-) dacites, pyroclasts, carbonatic sandstones and carbonates no extreme differences in the absorption features were detected between the different test areas (Fig. 5).
Some of the Mesozoic sandstones and most of the Neogene subvolcanic rocks (rhyolitic dacites) and related pyroclasts include kaolinized feldspatic or argillized components which caused stronger OH-absorptions around 1410 and 1920 nm in the mid IR. Depending upon the Fe2+, Fe3+, H_2O- and OOH-content of secondary mineral phases like hematite, limonite, jarosite or goethite (mostly in form of desert varnish) on many andesitic extrusiva, a wide and strong albedo decreases was observed over the near IR (946 to 855 nm), reaching a minimum in the visible blue/green (504 nm).
Due to the high amount of feldspatic and partly kaolinized/ argillized clasts almost every alluvial deposits (e.g. Quebradas) exhibit a moderate albedo in the visible (VIS) green/red (light brownish). The spectral properties of the Quarternary deposits (calcrete, salt pans) and Paleogene OH-rich alterations are well developed in the mid infrared (IR) near 1950 and 2350 nm. This energy absorptions are caused by the CO_3^{2-} -component of calcite (carbonates), the H_2O-component of gypsum and the OH-component of secondary clay minerals which represent the main mineral phases. Vice versa these minerals generate the highest albedos in the near IR between 1000 and 1500 nm.

Taking all measurements into account it is obvious that significant albedo and spectral signatures do occur in the near IR, the mid IR and to a certain degree in the VIS spectra. This emphasizes the importance of the TM bands 4, 5 and 7 if they are combined to a pure IR colour composite (CC) for the detection of alterations anomalies or if combined with one channel from the VIS to create a CC in which the general geology might be visualized.

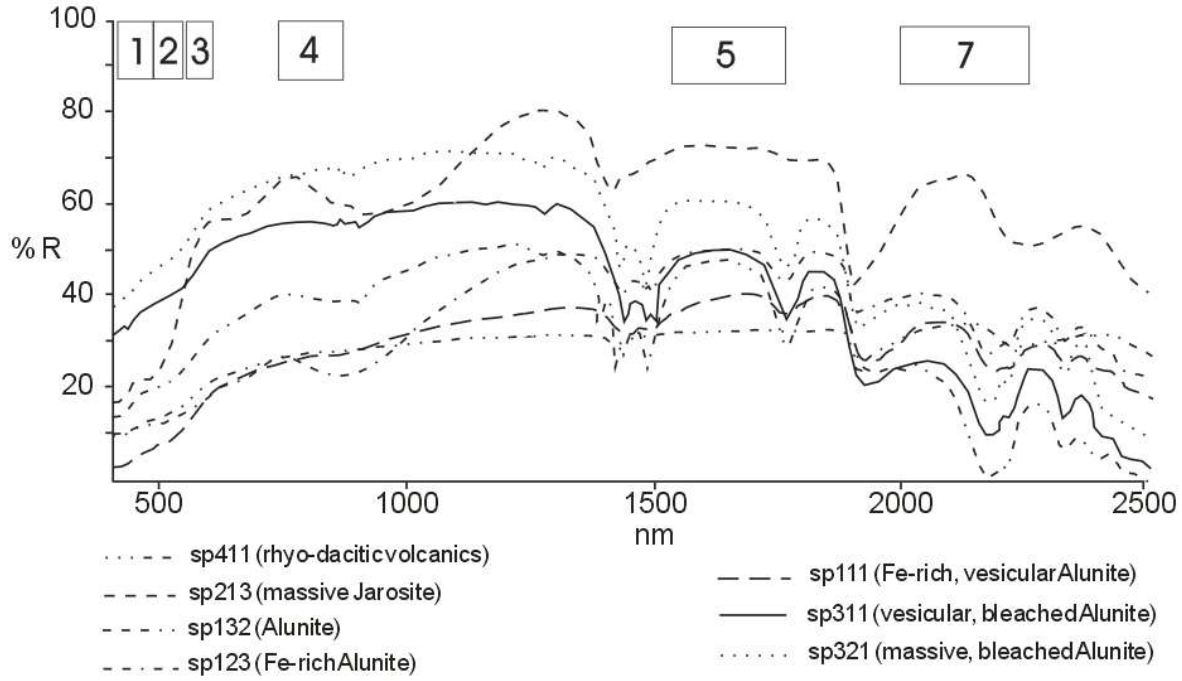

Fig. 5: Mean spectral features of some selected hydrothermally altered volcanic rocks of the test sites Indagua (I) and La Coipa (II) compared to the spectral TM sensibility over the region from 400 to 2500 nm.

4.2 Statistical analysis of the reflective TM data

What effects have the determined spectral properties for the statistical features of the selected TM data and how far is it possible to calculate an optimized CC without having the spectral information as a control (ASTER where not calculated since this scanner shows a similar uncorrelated wavelenght characteristic in the VIS/IR like the older Landsat MSS-system, but combined with a higher ground resolution of 15m/pixel)?

Table 1 shows the basic statistical parameters for all used reflective TM channels. The widest spectral variance occurs in the IR, especially in MBTM-5 and -7. MBTM-1 and -3 exhibit more or less the same DN standard deviations/variances (unlike MBTM-2 and -4). The spectral information of different TM bands is often strongly correlated (GRUNICKE, 1990; PRINZ, 1996), so it is necessary to evaluate their degree of correlation in order to determine least correlated channel combinations which might be suitable for the enhancement of destinct reflectance features. The strongest correlations exists within the VIS and IR spectra (Tab. 2) which can therefore be interpreted as two separate statitistical groups. Vice versa the lowest redundancy occurs between one dataset of the VIS and one dataset of the IR. Judging by this statistical analysis a combination of MBTM-1, -5 and -7 would represent the most uncorrelated pure CC.

Although this statistical method seems to be sufficient to select suitable TM bands for a CC it is also important to take the widest possible DN contrast into consideration which is also a criterion for the quality of the calculated image. CHAVEZ et al. (1980) developed the *Optimum Index Factor* (OIF) to evaluate the information content of any correlated dataset combinations. GRUNICKE (1990), BISCHOFF & PRINZ (1995) and PRINZ (1996) applied a modified OIF to the lithological analysis of TM and

TM-Channel	Dn_{min}	Dn_{max}	Dn_{mean}	σ	σ^2
MBTM-1	42	255	103.58	20.41	416.56
MBTM-2	14	255	55.01	14.09	198.52
MBTM-3	15	255	72.31	20.33	413.30
MBTM-4	7	255	63.41	18.99	360.62
MBTM-5	0	255	105.48	43.04	1852.44
MBTM-7	4	248	58.81	22.08	487.52

Tab. 1: Statistical parameters of the reflective TM data for the Maricunga Belt (MBTM) subscene.

MBTM	-7	-5	-4	-3	-2	-1
-7	*1.000*	0.972	0.891	0.869	0.829	0.679
-5	0.972	*1.000*	0.916	0.899	0.851	0.692
-4	0.891	0.916	*1.000*	0.984	0.937	0.817
-3	0.869	0.899	0.984	*1.000*	0.973	0.875
-2	0.829	0.851	0.937	0.973	*1.000*	0.948
-1	0.679	0.692	0.817	0.875	0.948	*1.000*

Tab. 2: Correlation (*r*) of the TM data for the subscene Maricunga Belt (MBTM), generated by a statistical analysis of the reflective DN values.

MSS multispectral data and achieved satisfying results for geological interpretation. The OIF is based on the DN correlation (*r*, representative for the uncorrelated information) and the spectral deviation (σ, representative for the expected DN contrast):

$$OIF = \Sigma \sigma_{(i)} / \Sigma |r_{(i)}|$$

(where i = amount of datasets/bands). The higher the OIF, the more uncorrelated spectral information is transformed into a contrast-rich CC. Table 3 shows the OIF-ranking of all possible three-channel combinations. Here the CC of MBTM-1, -5 and -7 is statistically defined as the most informative TM-dataset combination (OIF = 1). In this CC, most lithological classes are expected to be distinguishable by their different contrasts and special colour tones (note that the natural CC MBTM-3, -2, and -1 [rgb] contains a extreme low multispectral information; only rank 19!). So the OIF confirms the special spectral significance of the TM bands 5 and 7 for the lithological interpretation of CC's (see also cpt. 2.1). Furthermore, the OIF can be applied to any multispectral analysis, where no ground truth is available.

MBTM-CC	$\Sigma\sigma_{(i)}$	$\Sigma \lvert r_{(i)} \rvert$	OIF	Rank
157	85,53	2,34	36,55	**1**
135	83,78	2,47	33,92	**2**
145	82,44	2,43	33,93	**3**
357	85,45	2,74	31,17	**4**
125	77,54	2,49	31,14	**5**
457	84,11	2,78	30,26	**6**
257	79,21	2,65	29,89	**7**
345	82,36	2,80	29,41	**8**
235	77,46	2,72	28,48	**9**
245	76,12	2,70	28,19	**10**
137	62,82	2,42	25,96	**11**
147	61,48	2,39	25,72	**12**
127	56,58	2,46	23,00	**13**
347	61,40	2,74	22,41	**14**
134	59,73	2,68	22,29	**15**
237	56,50	2,67	21,16	**16**
247	55,16	2,66	20,74	**17**
124	53,49	2,70	19,81	**18**
123	54,83	2,80	19,58	**19**
234	53,41	2,89	18,48	**20**

Tab. 3: OIF-ranking for the possible CC's of the TM subscene Maricunga Belt (no colours are designated).

4.3 Colour Composites, ratios, principal components and classifications

OIF-defined colour composites may suppress reflectance features if they occur within small areas of the subscene, like alterations (due to the low number of pixels) because of their limited spatial extension. In such cases the special spectral properties of the target material has to be taken into account in order to select another sensitive band which might replace a band of broader sensitivity (or lesser interest for the detection of special alterations). Therefore the OIF defined CC of MBTM-157 (rgb) can be modified to the more specific OH-sensitive CC MBTM-457 (rgb) which has still a reasonable OIF-rank (rank 6) but is more target orientated. Furthermore all TM bands were chosen to calculate principal components (PC) and some sensitive ratios (R) in order to enhance these small scale features (DONKER & MULDER, 1976; GILLESPIE, 1980; PRINZ, 1996). Especially band rationing is an approved technique in order to emphazise the spectral features of minerals which are often bound to hydrothermal alteration zones (e.g. argillized minerals). Ratios of the TM bands 5/7, 5/1, 3/1 or 5/4 have been applied by many other authors in the past for the detection of OH-bearing secondary minerals (5/7), Fe-rich horizonts (5/1, 3/1) or silica-rich country rocks (5/4) of Au-, Ag- and Cu-deposits like the porphyry copper belts in Chile (ROWAN, 1977; ROWAN & KAHLE, 1982; SABINS, 1986; KAUFMANN, 1989; LOUGHLIN, 1991; PRINZ & BISCHOFF, 1995).

All of those single datasets can be combined to form hybrid CC's, which highlight strong reflectance differences, no matter how spatially limited they are. The important statistical criterion is the variance (σ^2) between each dataset (high variances are preferred for each component; see Table 4). Apart from the original TM bands 4, 5 and 7 the first three PC's and the three R's 5/4, 5/1 and 5/7 were calculated and later combined to form a hybrid CC with classified thematic overlays.

Component	σ^2	Component	σ^2	Component	σ^2
MBTM-4	360.81	MBPC-1	986.52	MBR-5/1	6.390
MBTM-5	1853.04	MBPC-2	113.33	MBR-5/4	289.20
MBTM-7	487.83	MBPC-3	82.53	MBR-5/7	157.25

Tab. 4: DN-variances of some selected MBTM, MBPC and MBR for the TM subset Maricunga Belt.

5.1 Indagua volcanic complex (test area I)

The Indagua test site is situated between the Qda. Indagua (W), the Qda. Colorada (NW) and the Qda. Cerros Bravos (SE) with the namegiving volcanic summit of the Cerro Indagua in its center. The general geology is characterized by sequences of Upper Jurassic to Lower Cretaceous (partly carbonatic) sandstones with some interbedded andesitic to basaltic lava flows (Fig. 6). In the southwest these sediments have been penetrated by a granodioritic intrusion (Cerro Dragon) followed by hydrothermally altered Upper Cretaceous to Paleocene pyroclastic rocks with flows of interbedded basaltic to (trachy-) andesitic lava which cover most of the northeastern parts of the investigation area. Around and northeast of Punta de la Aguja andesitic to dacitic subvolcanic domes crop out, showing some isolated appendices within the older pyroclastics. The Paleocene Co. Valiente volcanic complex consist out of (trachy-) andesitic lava flows originated from a subvolcanic intrusion forming the Co. Colorado in the north. Apart from this occurence the same volcanics can be found southwest of the Co. Indagua, seperated from the main outcrop by the Indagua Fault. In the center of the test area the Middle Eocene rhyodacitic subvolcanic dome and associated pyroclastics of the Co. Indagua volcanic complex can be considered as the main hydrothermal source (VÄTH, 1995). X-ray diffractometric analysis have given evidence that the different stages of alteration, defined by their typical mineral assemblages are characteristic for the 'acid sulfate type' as follows: Natro-alunite, kaolinite and vuggy silica (quartz) for the intensive alterations around the top of the dacitic dome, argillized minerals (clay minerals), kaolinite, partly chloritization and propylitic processes for the widespread moderate alterations. Sometimes associated with the latter type of alteration are hydrothermal carbonatic sinters and breccia dykes which can be found southwest/southeast of Co. Indagua. The youngest deposits are the alluvial fillings of the Quebradas and the debris of hydrothermally altered material along the slopes of Co. Indagua or the 'Indagua Fault' west of the summit (Mio- to Holocene).

Tectonically the area is dominated by SE-NW striking faults of which the most prominent fault is the 'Falla de Indagua' (Indagua Fault). VÄTH (1995) assumes by his own field observations that the fault caused a sinistral movement of about 1 km as indicated by the lateral displacement of the Cerro Valiente volcanics. This movement was triggered by a transpressional Eocene system, probably belonging to the 'Potrerillos-Maricunga Zone' (MPODOZIS et al., 1995). In addition many smaller

subparallel structures seem to have controlled the expansion of hydrothermal fluids which led to intensive silifications and brecciations (g.e. vuggy silica).

In order to determine the validity of remote sensing techniques for the alteration mapping of the study area, several multispectral image enhancing techniques were applied to the TM data. Most of the processed CC follow the OIF-defined combinations but some were additionally supplemented with band-ratios in respect to the spectral properties of indicative minerals. The images exhibit consistent relationships between the observed positiv albedo anomalies (high digital number = DN) and the surficial concentrations of OH-bearing minerals (e.g. alunite, jarosite) in hydrothermally altered rocks. Vice versa negative albedo anomalies (low DN) indicate different concentrations of iron oxides and hydroxides (e.g. hematite; goethite) in weathered surfaces with some implications for the composition of the countryrock. For example, the IR colour composite of the TM bands 457 (rgb) generally shows iron oxides in variations of blueish and reddish colours, green vegetation as deep red and argillic alterations as bright green, yellow or white.

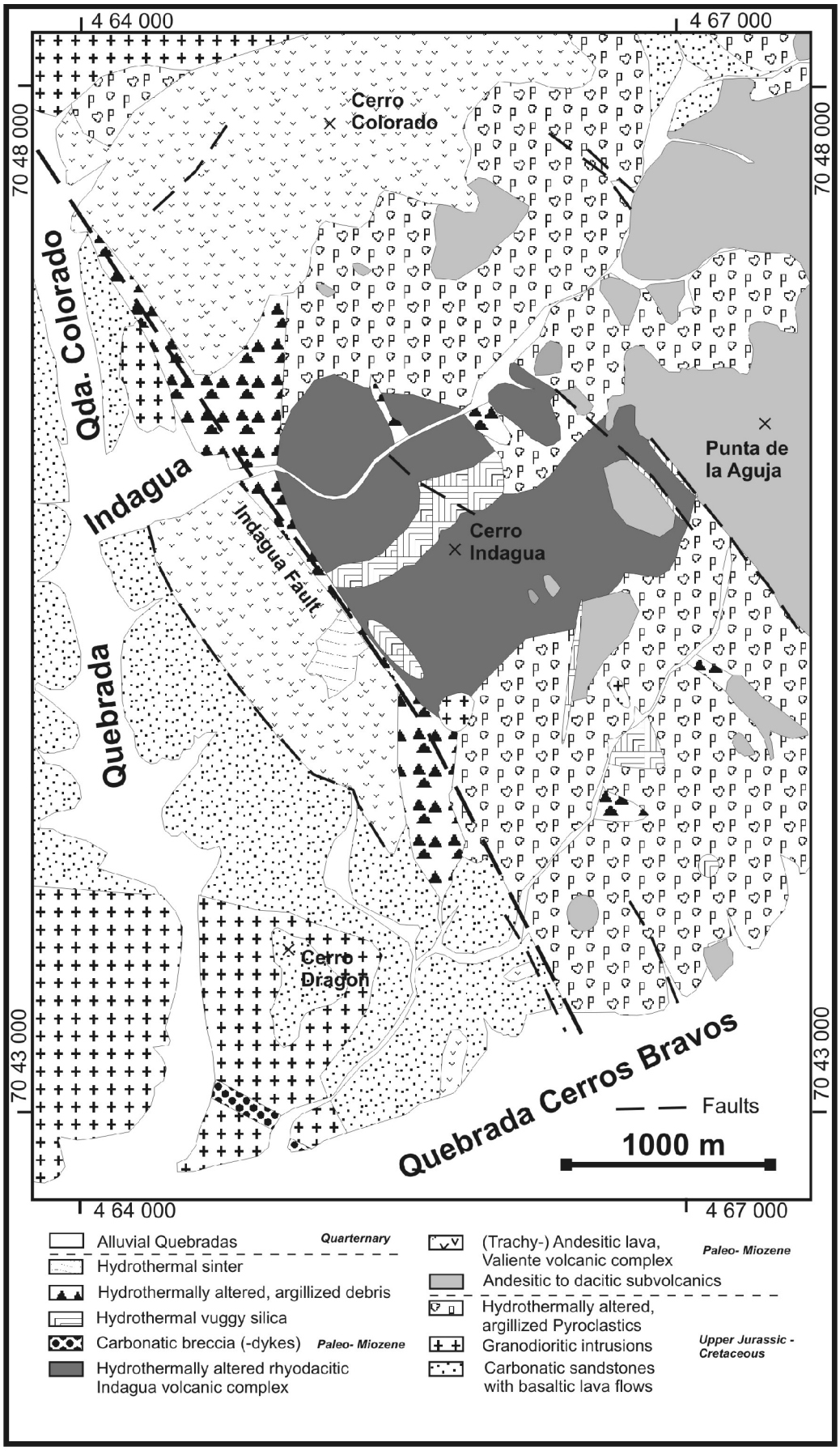

Fig. 6: Geological scetch map of the Indagua test site showing the major lithological classes as revealed by field and multispectral remote sensing studies (modified after VÄTH, 1995).

However, in some altered areas the extreme albedo effects of the argillized, partly silicified outcrops of clay mineral-rich volcanics (highest albedo in all bands) dominate the total brightness of the Indagua subsccene. Thus, the critical alteration zones occur as white surfaces with some marginal influences of yellow or blue, depending on the local mineral composition (Fe-low dacites/pyroclastics vs. Fe-rich andesites/basalts). Figure 7 shows the area of Cerro Indagua as an infrared CC MBTM-457 (OIF rank 6), which allows a fair approximation of the different types of rock and the detailed mapping of some extensive alteration zones within the test site.

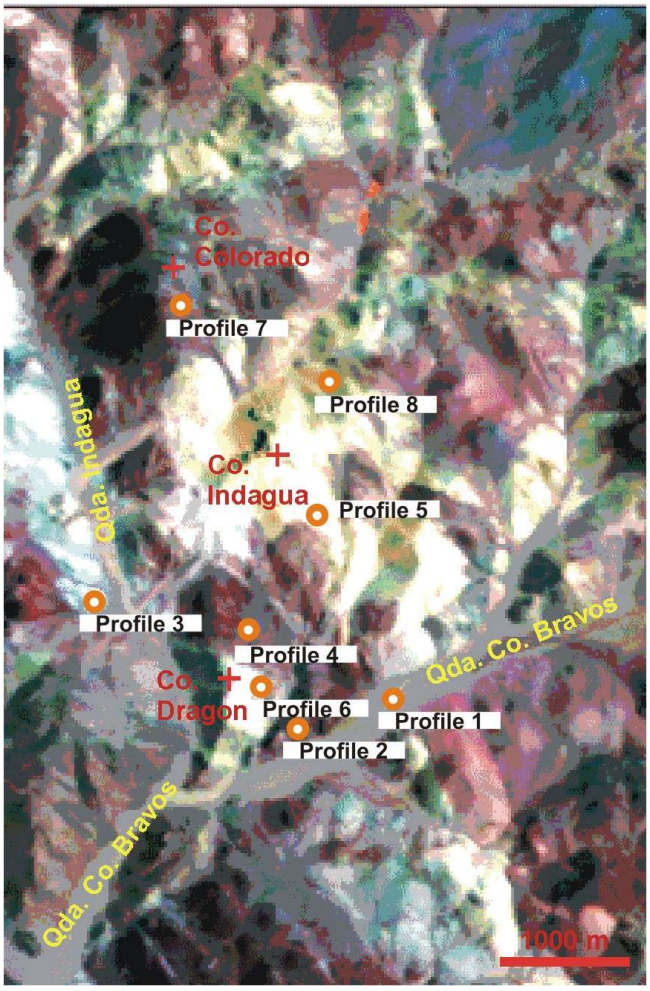

Fig. 7: Infrared colour composite (MBTM-457 → rgb) of the Indagua test site, displaying the locations of selected spectral profiles referring to important lithological classes. Alterations and carbonatic rocks can easily be identified by their outstanding strong IR-reflectance (high DN value = bright pixel clusters).

In addition the location of some selected spectral profiles are indicated; each profile corresponding to a lithological class as follows: Alluvions (profile 1), red sandstones of the Qda. Monardes Fm. (profile 2 and 4), carbonatic sandstones of the Pedernales Fm. (profile 3), intensive argillized pyroclastics and rhyodacites of the Cerro Indagua volcanic complex (profile 5 and 6) and the andesitic volcanics of the Cerro Valiente volcanic complex (profile 7). The highest albedo in form of pixel values (DN) occur in band 5 (IR) at profile 3, 5 and 6 (Fig. 8), all situated in the hydrothermally altered (rhyo-) dacites/pyroclastics of Cerro Indagua or within the carbonatic sandstones of the underlying Pedernales Fm.. Although this observations is based on a rough

albedo interpolation between six isolated DN-measurements (TM bands), the continuous laboratory reflectance spectra of representative rock samples (Fig. 5) proves that most of the selected samples are either alunite, derived out of altered subvolcanic rocks or sandstones with a calcitic matrix. Due to the lower absorption features of calcite in the spectral region of TM band 7 compared to those of alunite, blueish/greenish shades within the white areas of the IR image MBTM-457 (rgb) indicate the non-altered sandstone areas, whereas the OH-bearing minerals (alunite!) lead to a light yellow colour tendence around the hydrothermally altered volcanics of the Cerro Indagua complex. Looking south from its summit the smaller Cerro Dragon, which is basically an intrusion of granodioritic magma into the sandstone sequences of the Pedernales and Monardes Fm. (VÄTH, 1995), exhibits similar albedo features.

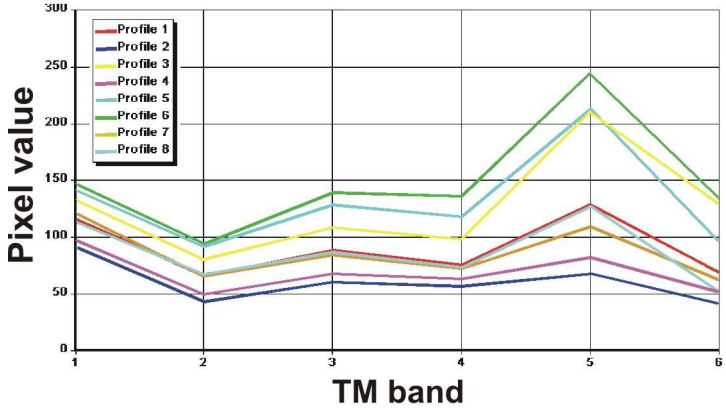

Fig. 8: Extrapolated spectral profiles of important lithological classes over the TM band sensibility (6 = band 7) within the Indagua test site (for locations see figure 7). The highest albedos (here: DN/pixel value) are corresponding with hydrothermally altered pyroclastics and carbonatic sandstones.

Applying a surface profile based on TM band 5 from the alluvial Qde. Cerros Bravos to the southwestern slopes of Cerro Dragon (Fig.9) the high IR response of spacially limited outcrops of a hydrothermal carbonatic breccia dyke and an erosional remnant of carbonatic Pedernales sandstones are easily to distinguish from the surrounding granodioritic rocks by their unusual high DN values.

To overcome the common problem of varying scene brightness due to different illumination angles caused by a dynamic geomorphology additional band rationing were applied to selected TM bands. These ratios also accentuate the spectral signature curves of indication minerals like alunite (Fig. 5) in hydrothermally altered areas (DRURY, 1987; SINDERN et al., 1995; PRINZ & BISCHOFF, 1995). If the TM bands used are chosen to cover reflectance peaks, absorption troughs and changes in slope on the curve like band 3, 1, 5 , 7 or 4, then they can be combined in pairs as ratios to express the spectral signature of the critical material. MBR-5/7, MBR-5/4 or MBR-3/1 are some of those ratios which enhance the spectral signatures of OH-bearing minerals in hydrothermal altered rocks, especially those of alunite, kaolinite, carbonates (calcite) or iron oxides/hydroxides like hematite/jarosite. Figure 10 displays the CC MBTM-457 (rgb) with an additional overlay in blue, based on a supervised maximum likelihood pixel classifiction of the ratio MBR-5/7 indicating OH-sensitive mineral surfaces of the Indagua area. The remarkable well fitting boundaries of both layer types referring to the hydrothermal alteration zones (while excluding the carbonatic sedimentary rocks west of the Qda. Indagua!) underlines the

efficiency of this image processing technique in order to map potentially mineralized surfaces. A comparison with the sketch map (Fig. 6) indicates that hydrothermally altered areas around Co. Indagua are spectrally anomalous and there are further anomalies north and south of it representing locations of future prospects (like north of Co. Colorado or south of Qda. Co. Bravos).

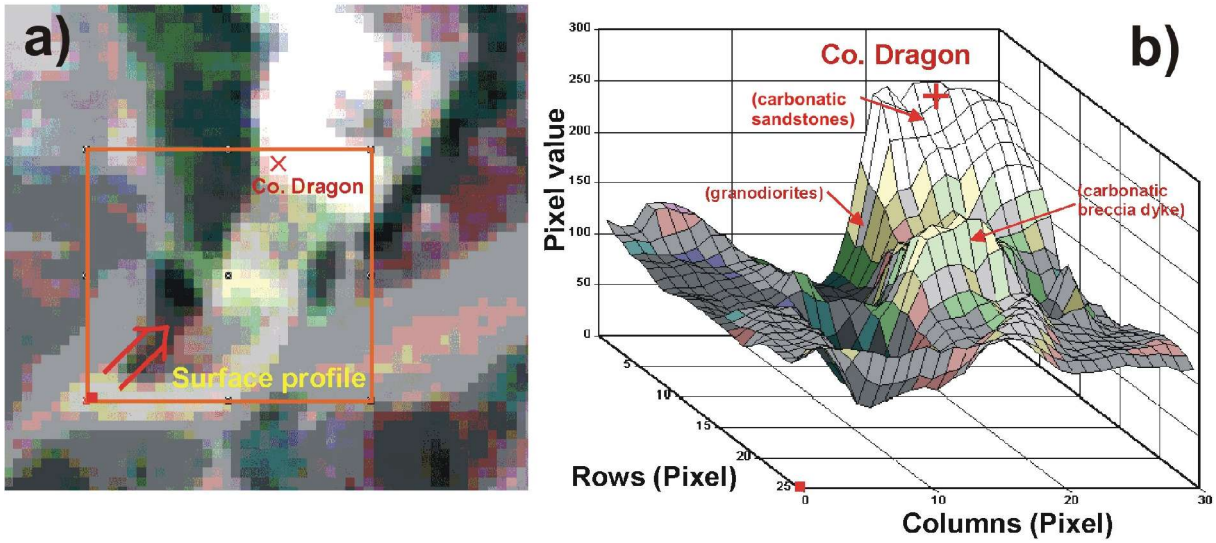

Fig. 9: Orientation of a spectral surface profile (a) southwest of Cerro Dragon (Indagua test site, red box indicates the point of perspective view) applied to MBTM-5 and its 3-dimensional expression combined with the IR overlay MBTM-457 (rgb), exhibiting the high IR albedo of hydrothermally altered rocks, carbonatic rocks and carbonatic volcanic breccias (b).

One of the most sophisticated image enhancing techniques is the calculation of principal components (PC's) of the analysed multispectral TM data set (LOUGHLIN, 1991). Depending on the covariance and correlation of the TM DN-values, six new datasets were calculated, each showing a different eigenvector-loading from the original bands depending on their spectral sensibility. A CC (fig. 11) of the first three principal components (MBPC-123 [rgb]) reveals the mineral diversity of the detected alterations around Cerro Indagua much more detailed than ratios or original bands would do. The main reason for this fact is the compressed multiple spectral information in each PC (DRURY, 1987; LOUGHLIN, 1991): The 1rst PC generally represents the total albedo of all involved bands, the 2nd PC represents the main spectral differences between the VIS and IR spectra whereas the 3rd PC can be taken as an approximation of the internal spectral differences within the IR. The remaining three PC's (4th, 5th and 6th) can be considered to contain diverse information due to the varying spectral response of objects with a lower 'spectral weight' (extreme: transmission noise!). It follows that the IR-sensible alteration zones of the Indagua investigation area should therefore be displayed in a more colourful composite caused by the increasing albedo variance between the VIS/IR properties by using PC's.

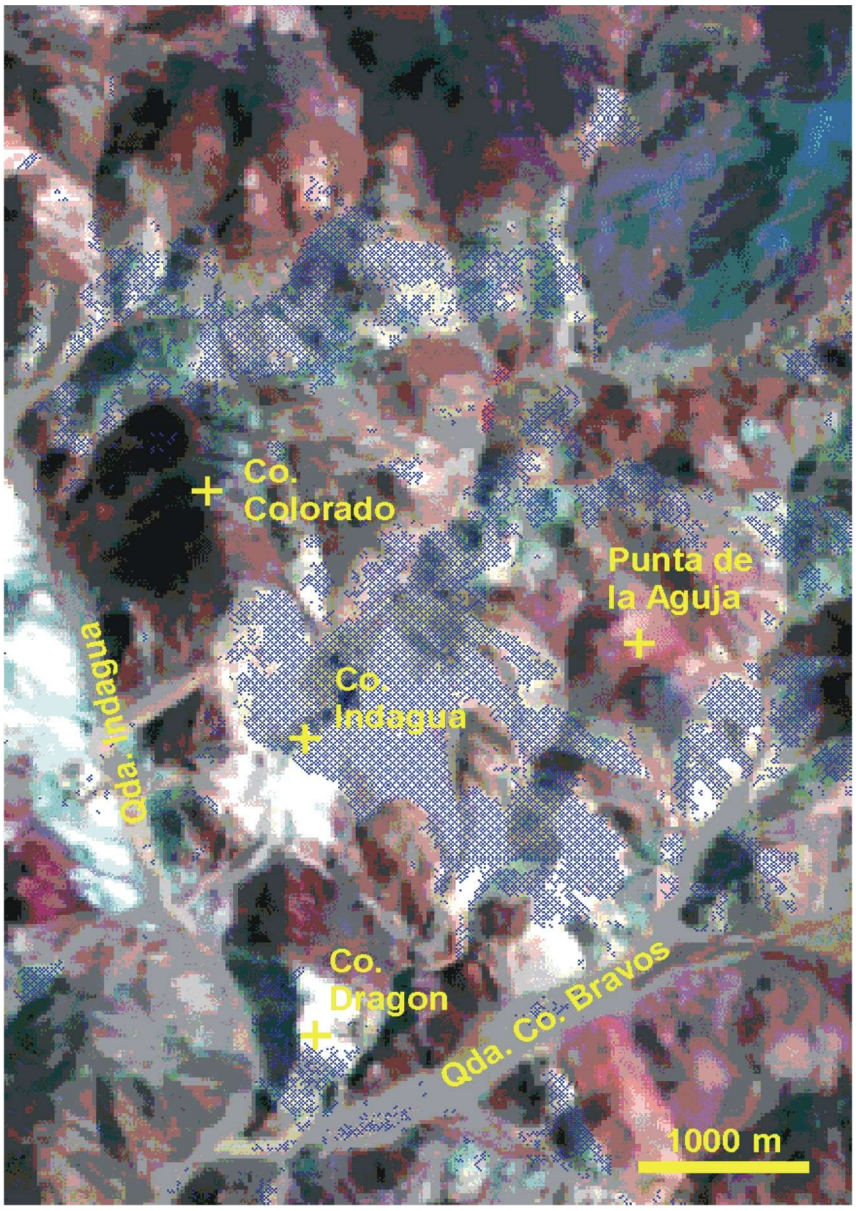

Fig. 10: The Indagua test site displayed in the OIF qualified CC of MBTM-457 (rgb) in combination with a classified OH-sensitive ratio MBR-5/7, indicating OH-rich hydrothermally altered surfaces around Co. Indagua and other locations in blue, while excluding the carbonatic sediments of Cerro Dragon or similar rocks west of the Qda. Indagua.

Summarizing all the above, we can state that iron-oxides, -hydroxides are mapped into the PC-composite in dark brown to greenish colours (andesitic and pyroclastic surfaces), due to the fact that virtually all rocks and soils are affected by iron-oxide staining to some degree (desert varnish!) and their albedo contribution are low in all three PC's. Their OH-specific spectral features are masked and dominated by the argillic minerals or silica-caps even in higher PC's, where hydroxyls should theoretically have a higher reflectance (positive eigenvalue from MBTM-5 for both types of mineral). Carbonatic sandstones are expressed in bright turquoise (west of Cerro Dragon), unaltered dacitic to rhyodacitic subvolcanics in medium to dark olive-green, granodioritic intrusions in grass-green to brownish green (around Cerro Punta del la Aguja and north of Cerro Colorado). For alteration mapping MBPC-123 (rgb) indicates areas where rocks and soils are liable to argillization as follows: bright pink pixels represent inferior argillized zones around granodioritic intrusions (Cerro

Dragon), while purple to deep blueish pixel clusters represent areas of intense hydrothermal alterations, e.g. around Cerro Indagua or along its western slopes, subparallel to the important SE-NW striking Falla de Indagua.

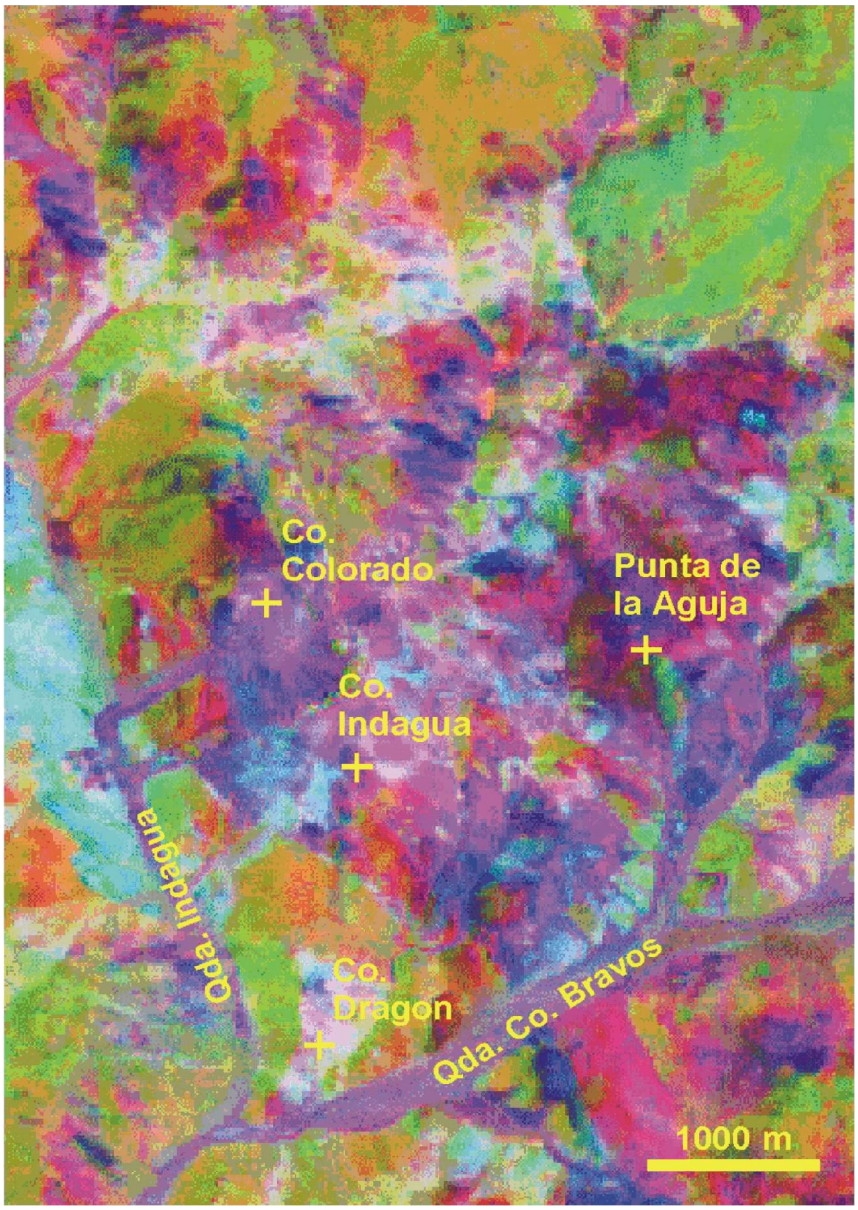

Fig. 11: The Indagua test site displayed as CC of the first three principal components (MBPC-123 → rgb), allowing a more detailed discrimination of different kind of lithologies and alterations. OH-rich hydrothermally altered surfaces around Co. Indagua are expressed in blueish to pink/purple colours, carbonatic sediments are defined by turquoise pixel clusters, unaltered volcanics are displayed in greenish to brownish colours.

Among all lithological classes any kind of mixed pixels (= 'mixel') can be observed, especially in areas of intense meso- to epithermal alteration (Cerro Indagua complex) because the recognition of such mainly argillized surfaces is often encountered by additional silicification and iron-staining of the same rock. LOUGHLIN (1991) states that these zones may be detected at deeper erosion levels in mesothermal systems and as the dense siliceous caprock is often associated with epithermal mineralization. These mixels may also lack typical iron-oxide signatures in the visible spectra due to the overprint by highly reflective argillic minerals such as kaolinite. Applying an OH-

and Fe/CaCO-sensitive overlay (pixel classification of MBR-5/4; MBR-5/7) to the CC (latter one transformed into a 256 DN greytone image for better significance!) it becomes clear how accurate the PC-method is for the test site (Fig. 12).

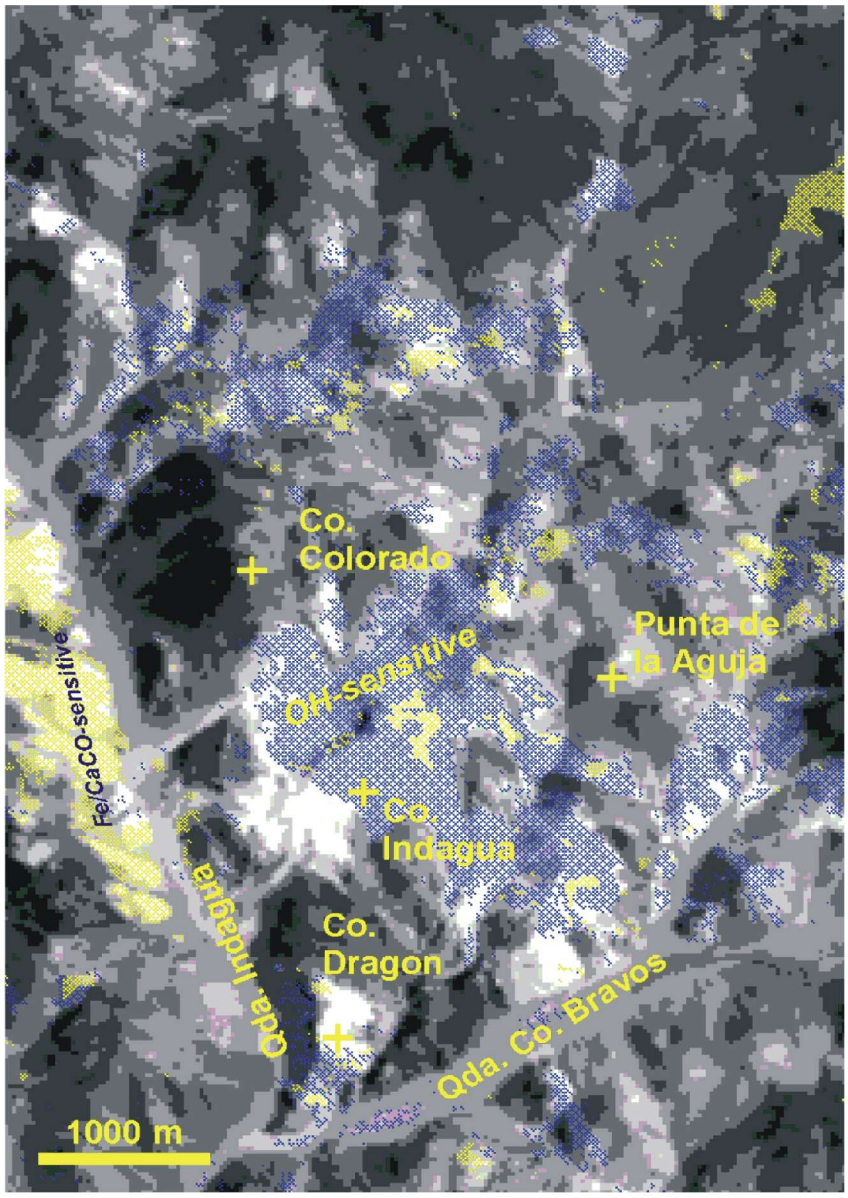

Fig. 12: The Indagua test site displayed as MBPC-123 (256 grey tones) in combination with the classified OH-sensitive ratio MBR-5/7, indicating OH-rich hydrothermally altered surfaces around Co. Indagua and other locations in blue and the classified Fe/CaCO3-sensitive ratio MBR-5/4 mapping carbonatic rocks in yellow (Cerro Dragon or west of the Qda. Indagua).

5.2 La Coipa (test area II)

The La Coipa test site is situated southwest of the volcano Cerros Bravos, between the Qda. La Coipa in the south and the Cerro Vicuña in the north (SINDERN et al., 1995). In this zone the open pits of La Coipa and Can Can represent two of the biggest epithermal precious metal (Au, Ag) deposits in Chile. The genesis of these deposits are spatially and temporally related to Lower Miocene volcanic activities (OVIEDO et al., 1991) and its associated hydrothermal alterations of mainly pyroclastic rocks which are the predominant type of rocks (Fig. 13).

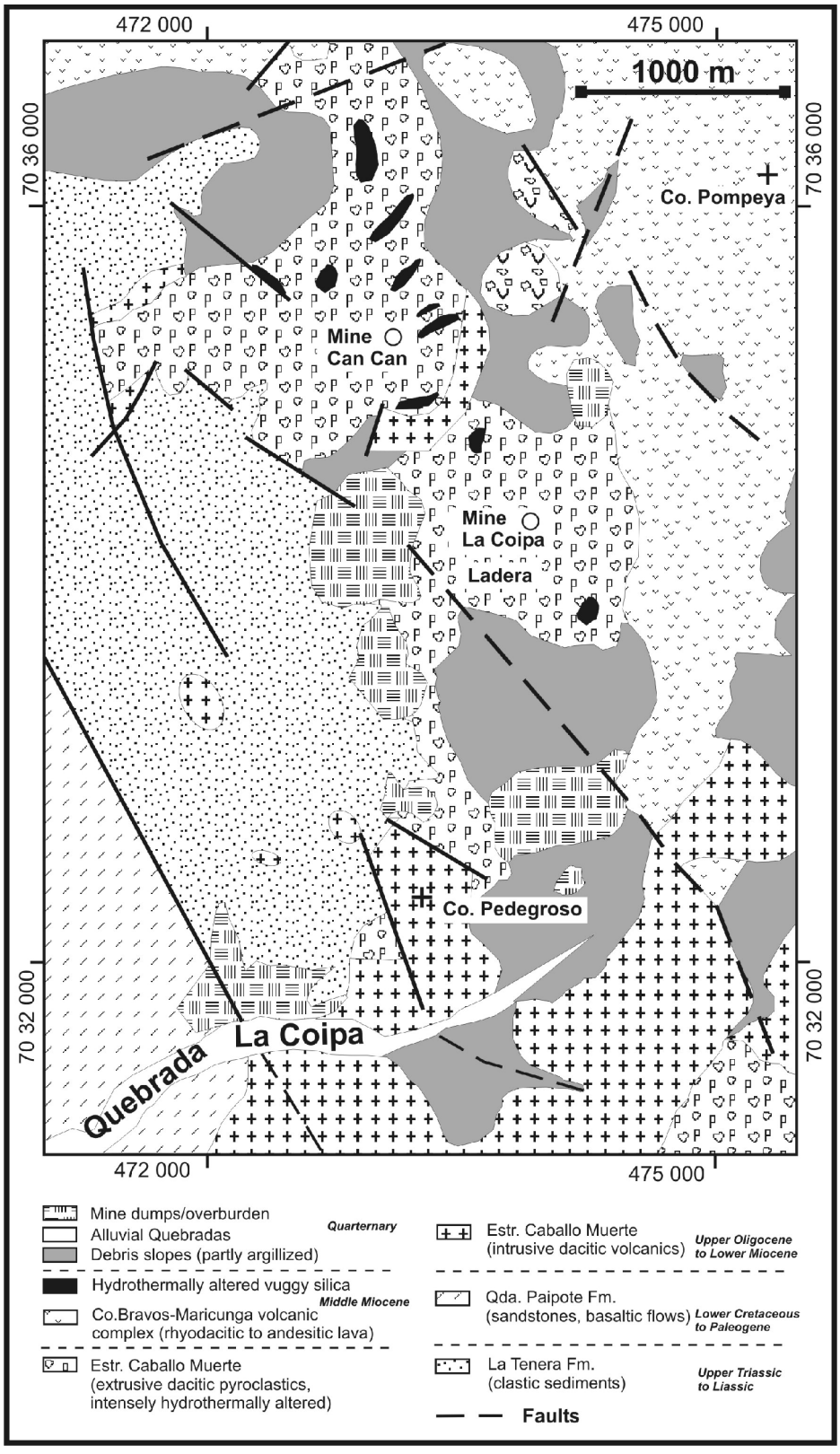

Fig. 13: Geological scetch map of the La Coipa test site showing the distribution of major lithological classes as revealed by field and multispectral remote sensing studies (modified after SINDERN, 1993 ; HELLEBRANDT, 1993).

Outcrops of Permian granites (Caballo Muerto granite) represent the local basement, which is covered by Upper Triassic to Jurassic silt- and sandstone sequences of the La Tenera Fm.. Basaltic Flows and coarse clastic units of the Upper Cretaceous to

Paleogene Quebrada Paipote Fm. are restricted to the southwest of the investigation area. The younger Upper Oligocene to Lower Miocene Estratos de Caballo Muerto can be devided into the dacitic intrusions of Paloma, Can Can, Pedregoso and La Coipa (where SINDERN et al. [1995] distinguished more then six different dacitic units and related rhyolitic dykes) and the associated altered pyroclastics/dacitic lava flows of the La Coipa sequence. The occuring type of hydrothermal alterations are similar to those described for the Indagua test site (acid-sulfate type) but are more intensive in some localities, representing the definite source of ore enrichment. Especially the porous pyroclastics and the underlying siltstones of the La Tenera Fm. were strongly influenced by the hydrothermal fluids. The shape of the alteration zones are controlled by subvertical faults, showing mainly a NE-SW orientation (expressed by the striking of the many vuggy silica dykes) whereas the total alteration area between Ladera Farallon and Coipa Norte shows a more N-S- elongation according to the dominant regional system. In addition some subordinate NW-SE striking tectonic structures are developed as normal faults, assosiated with minor hydrothermal alterations (SINDERN, 1993). Extension at these fractures were caused by dextral movements along the NNE-SSW striking major faults of the northern Maricunga Belt (SINDERN et al., 1996). Younger local NW-SE orientated normal faults caused a further subsequent displacement of the alteration zones.
East of the La Coipa mining district the Middle Miocene Cerros Bravos-Maricunga Volcanic complex comprises one trachy-andesitic to trachy-dacitic intrusion and five andesitic to rhyolitic extrusive units. The Quebradas and most of the steep mountain slopes are covered with loose gravel and volcanic debris of Quarternary age or in case of the open pit La Coipa (Falleron-Ladera), with huge amounts of anthropogene mining dump material.

The remote sensing analysis of the La Coipa mining district exhibits similar spectral anomalies for the majority of the mapped or presumed alterations compared to the features of the Indagua area (see above). Based on the OIF-defined IR false colour composite MBTM-457 (rgb) several reflectance profiles (Fig. 14 and Fig. 15) were taken, corresponding to important lithological classes. The spectral profiles 7 (intensive argillized to silicified pyroclastics of Cerro La Coipa) and 4 (intensive argillized to silicified pyroclastics of the dacitic La Coipa complex) exhibit the highest albedo features, especially in TM band 5. These observations are consistent with the laboratory spectra of representativ samples in the IR (Fig. 5) and their visible albedo features in the field (Fig. 16). The lowest reflectivities are indicated by profile 1, 5 and 6 (basaltic to andesitic lava and unaltered dacitic rocks of the La Coipa complex), whereas the partly altered dump material of the mines and carbonatic sediments of the Qda. Paipote Fm. and La Tenera Fm. show a moderate albedo (profile 2 and 3). Figure 17 confirms how well the intensely altered rocks of the La Coipa complex are visualized by the IR composite MBTM-457 because an applied coverage of SiO/Fe- and OH-sensitive ratios (MBTM-5/4, MBTM-5/7) coincides precisely with these spectral anomalies. More than this the two ratios can also be applied to the further discrimination of sedimentary-hosted spectral anomalies due to the high content of quartz, iron and carbonate in the sand- and siltone sequences of the La Tenera Fm. (5/4) from the important volcanic-hosted hydrothermal OH-bearing alterations of the dacitic La Coipa complex (5/7).

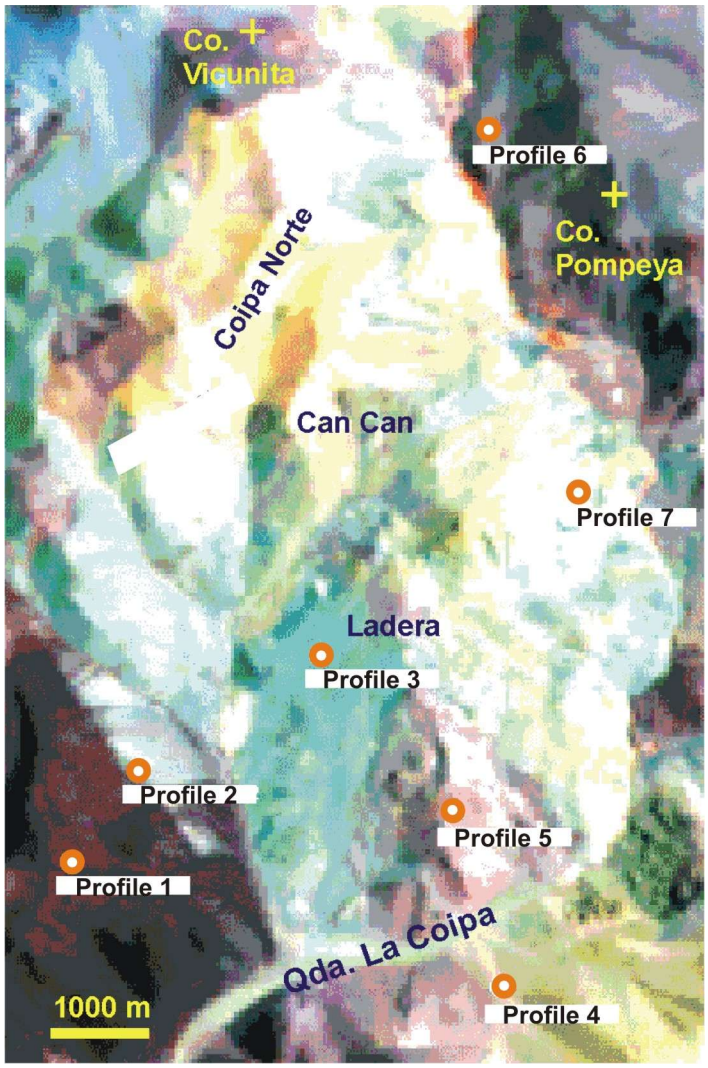

Fig. 14: Infrared colour composite (MBTM-457 → rgb) of the La Coipa test site, displaying the locations of selected spectral profiles refering to important lithological classes. Major alterations and minor carbonatic sediments can easily be identified by their outstanding strong IR-reflectance (high DN value = bright pixel clusters) leading to white, yellow or turquoise colours.

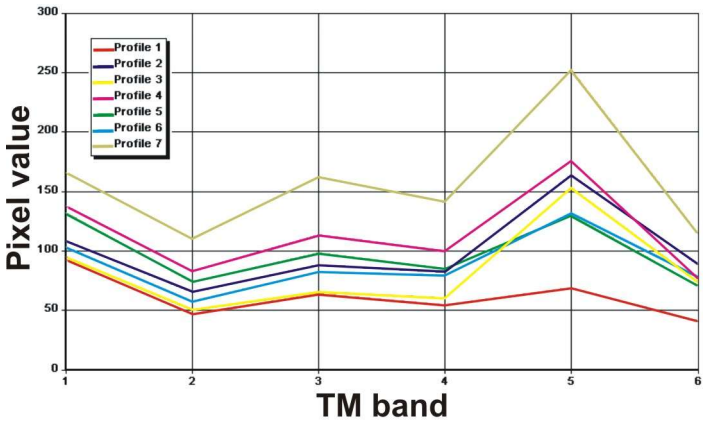

Fig. 15: Extrapolated spectral profiles of important lithological classes over the TM band sensibility (6 = band 7) within the La Coipa test site (for locations see figure 7). The highest albedos (here: DN/pixel value) correspond with hydrothermally altered pyroclastics and beds of carbonatic silt-/sandstones.

Unfortunately the weathered mining dumps southwest of the open pits Can Can, Margarita and La Coipa Norte response in the same spectral OH-sensitive way, so one has always to consider the possible anthropogene influences on the mapped albedo features.

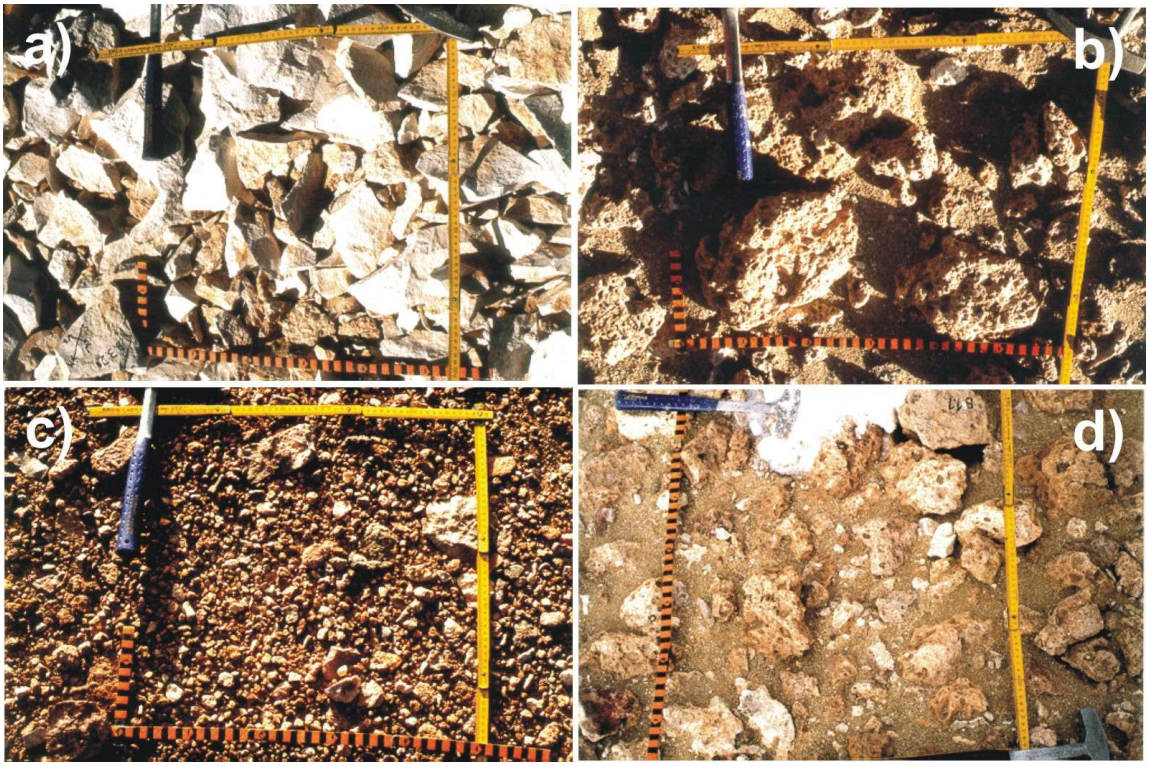

Fig. 16: Hydrothermally altered and partly bleached Neogene pyroclastics of Can Can and La Coipa: a) massive alunite; b) bleached, porous alunite; c) jarosite-rich debris and d) vuggy silica (quartz).

For the further discrimination of the detected spectral anomalies the first three principal components were combined to form a false colour composite (Fig. 18) with special interest on the altered surfaces around Can Can, south of Cerro Vicuñita. Regarding to HELLEBRANDT (1993) und SINDERN (1993) the pyroclastics and different dacitic intrusions are characterized by an intense hydrothermal alteration of silicic to clay-mineral rich type. The characteristical alteration minerals are quartz and kaolinite, in some place so concentrated that they form elongated bodies of brecciated vuggy silicas. These strongly altered zones are easy to map in the PC image, because they show the highest DN in PC-1 (high total albedo of quartz over the entire TM spectra!), causing a reddish/purple pixel signature in MBPC-123 (rgb). The less silicified zones are characterized by turquois to greenish colours, due to the high eigenvector-loading of DN values of OH-bearing materials in PC-2. Both type of alterations lead to mixels clusters of blueish to purple colour. Non-altered surfaces are displayed in brown or olive-green colours.

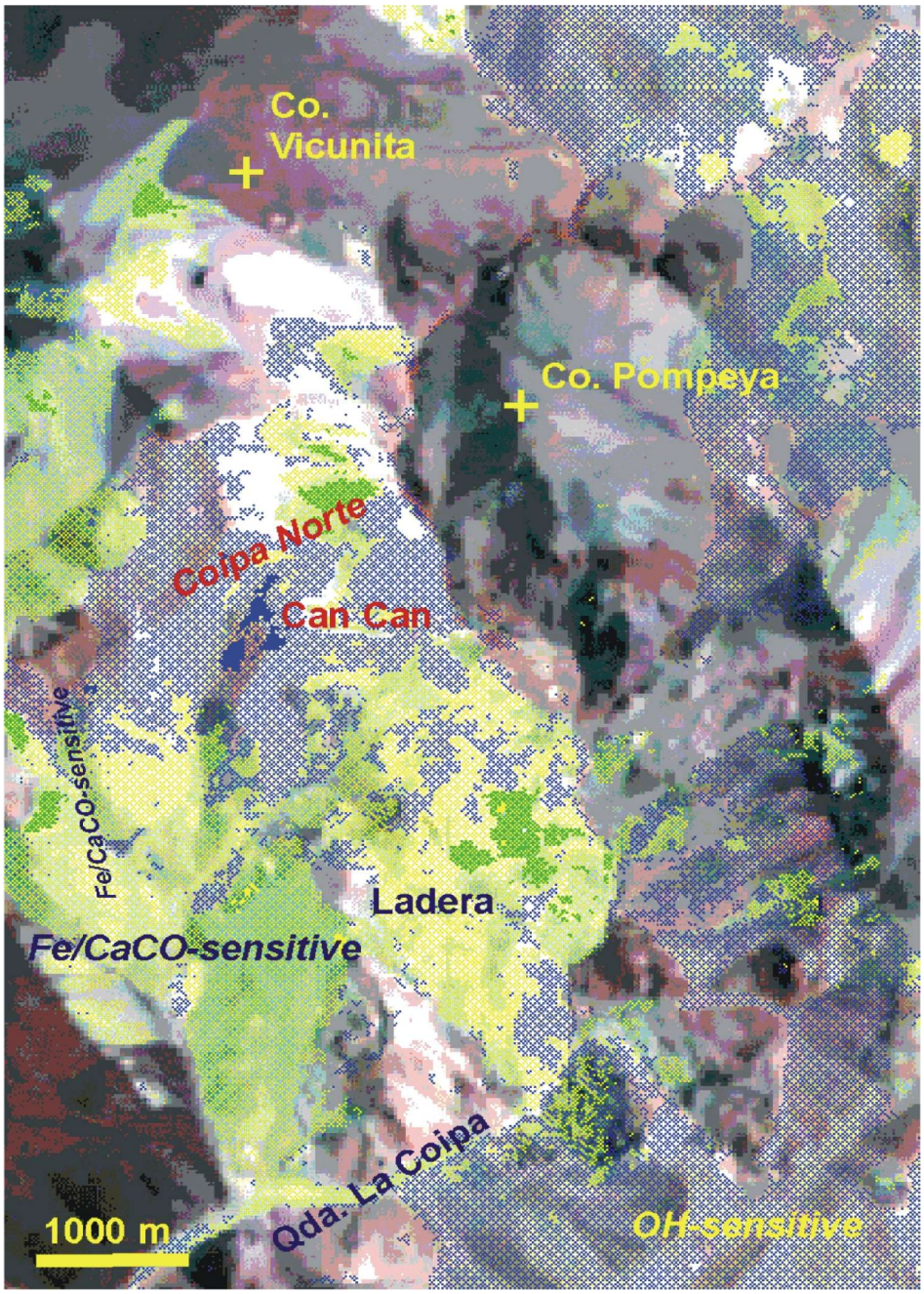

Fig. 17: The La Coipa test site displayed in the OIF qualified CC of MBTM-457 (rgb) in combination with a classified OH-sensitive ratio MBR-5/7, indicating OH-rich hydrothermally altered surfaces around Can Can and Coipa Norte in blue. The classified Fe/CaCO-sensitive ratio MBR-5/4 shows its corresponding pixel clusters in green to yellow colours (e.g. Ladera and other locations more westwards).

Most detected signatures are so distinct that these anomalies can be extrapolated to the southeast in direction of the Paloma mining region, based on additional FeOH-, OH- and CaCO-sensitive classified ratio overlays (Fig. 19) . The type of presumed alterations are consistent with the field observations of HELLEBRANDT (1993), who described more than five different kind of OH-mineral-rich alterations, also including vuggy silicas. Latter ones are gernerally hard to detect because of their small dimensions and similar albedo features to silicic or argillized dump material in common CC's. Combining the three components PC1, MBR-5/4 and MBTM-5 (rgb) to a hybrid CC allows the seperation of some vuggy silica dykes southeast of the

mine Can Can (Fig. 20) by their outstanding bright albedo (white pixels) within the more purple coloured areas of argillized, hydrothermally altered pyroclastics.

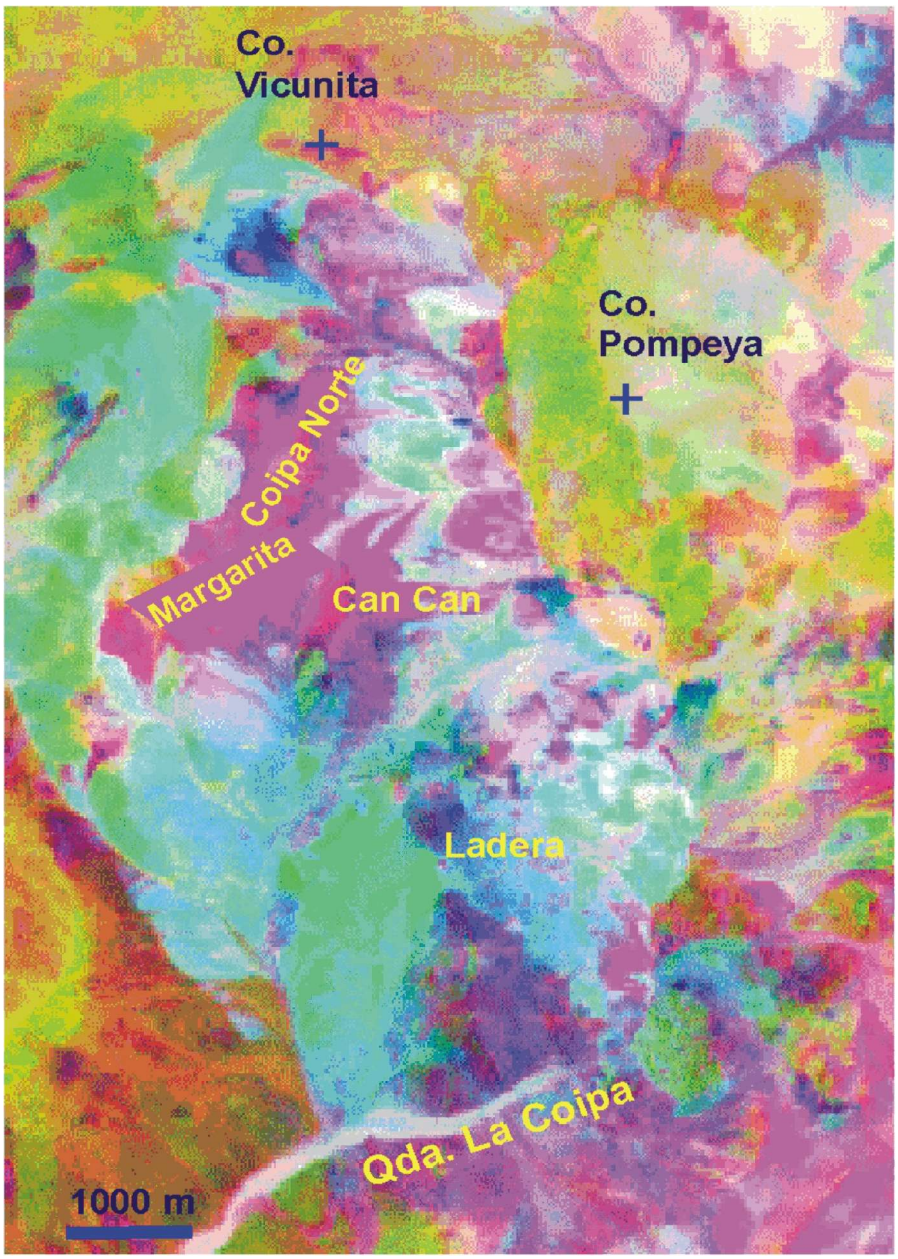

Fig. 18: The La Coipa test site displayed as a CC of the first three principal components (MBPC-123 → rgb), allowing a more detailed discrimination of different kind of lithologies and alterations. OH-rich hydrothermally altered surfaces of Can Can and Ladera (mine La Coipa) and south of Qda. La Coipa (Paloma) are expressed in blueish to pink/purple colours, carbonatic sediments are defined by turquoise pixel clusters, unaltered volcanics are displayed in greenish to brownish colours (e.g. Co. Pompeya).

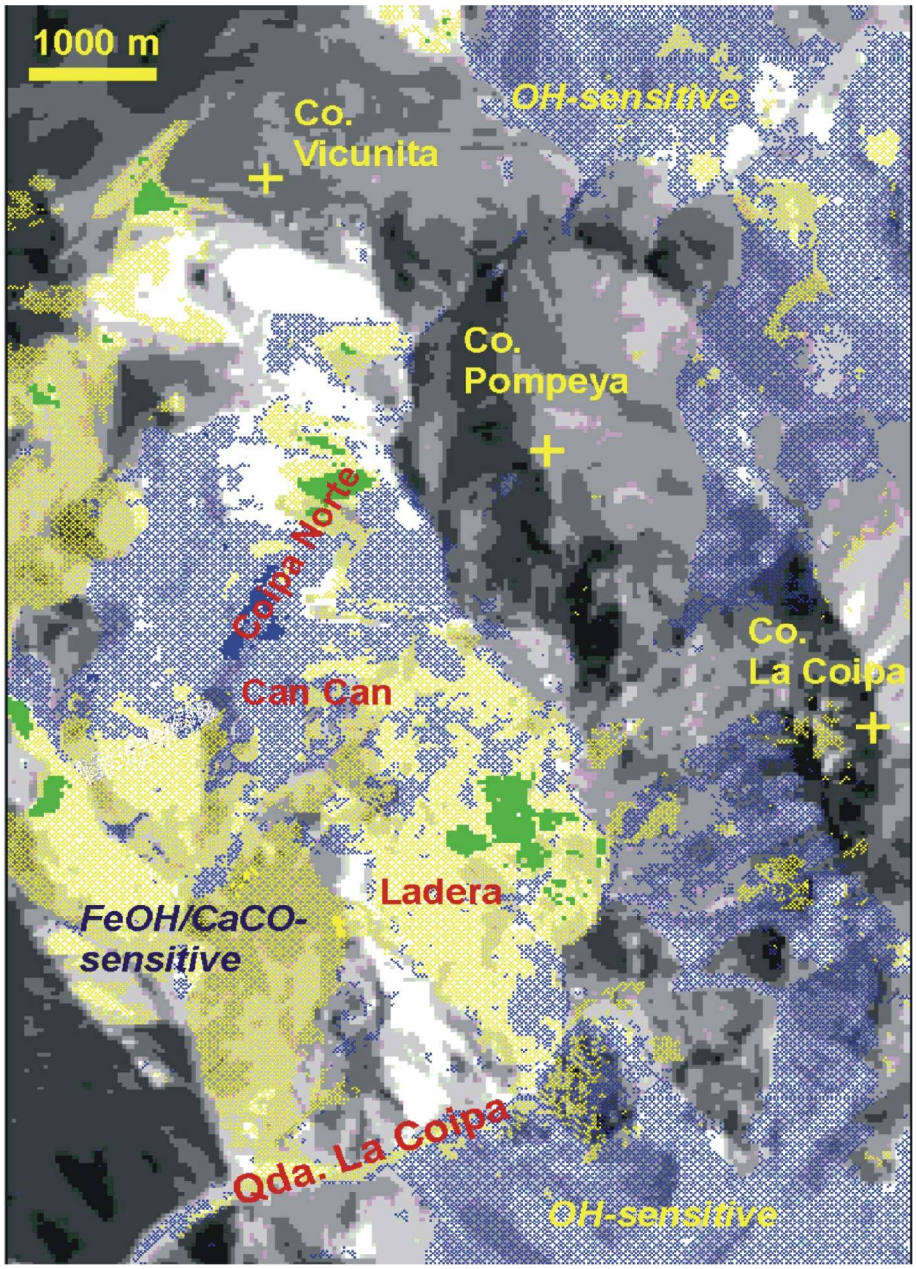

Fig. 19: The La Coipa test site displayed as MBPC-123 (256 grey tones) in combination with the classified OH-sensitive ratio MBR-5/7, indicating OH-rich hydrothermally altered surfaces around Can Can/Coipa Norte and other localtions in blue while the classified Fe/CaCO-sensitive ratio MBR-5/4 mapps carbonatic and FeOH-rich rocks in green to yellow (e.g. Ladera or northwest of the Qda. La Coipa).

5.3 Extrapolation of the remote sensing results

Based on the results of the remote sensing analysis more than 20 hydrothermal alteration zones of different dimensions can be located within the entire TM subset (see also appendix map 1):

1. Center near UTM 458/7070. Two medium sized alterations in the vicinity of the abondened mine El Mondimiento (max. extension 300 x 1000 m).
2. Center near UTM 457/7065. Group of two small to large sized alterations around Co. El Hueso (max. extension 1000 x 2500 m).

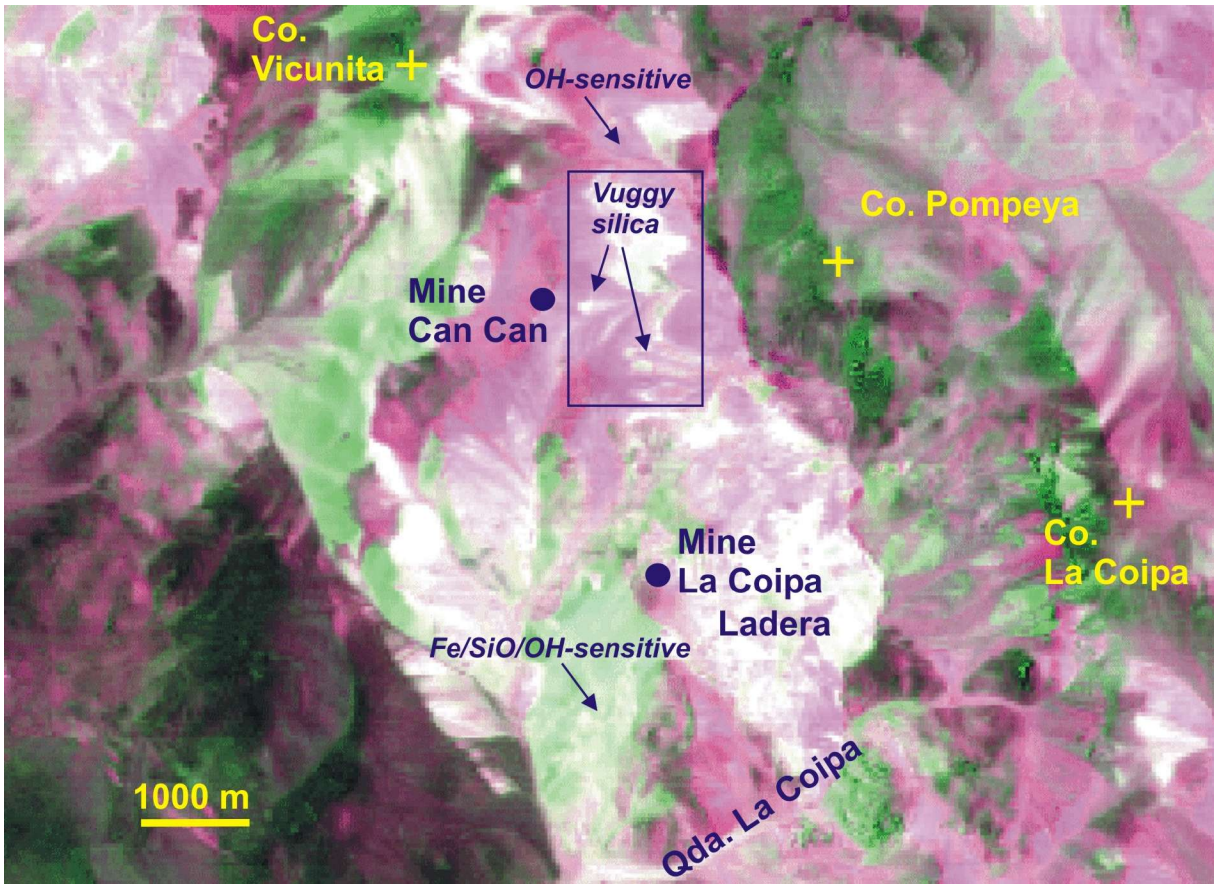

Fig. 20: The La Coipa test site displayed as a hybrid CC of MBPC-1 in combination with MBTM-5 and MBR-5/4 (rgb), expressing OH-rich hydrothermally altered surfaces around Can Can/Coipa Norte and similar altered surfaces in pink while the small vuggy silica 'dykes' southeast of Can Can can only be detectet by their different, overall bright albedo in all chosen components if not masked by weathered dump material or silicified debris.

3. Center near UTM 461/7069. Group of small to large sized alterations around Co. Silica (max. extension 500 x 1000 m).
4. Center near UTM 460/7063. Group of four medium sized alterations southeast of Co. El Hueso (max. extension 1500 x 2500 m).
5. Center near UTM 463/7059. Group of two smaller alterations southeast of Qda. La Cuesta (max. extension 500 x 800 m).
6. Center near UTM 462/7055. A medium sized alteration west of Co. Bandera (max. extension 100 x 1500 m).
7. Center near UTM 466/7058. A medium sized alteration east of Qda. Larga (max. extension 100 x 1200 m).
8. Center near UTM 467/7055. Group of two smaller alterations southwest of Co. Bravos Negros/end of Qda. Larga (max. extension 100 x 500 m).
9. Center near UTM 474/7057. Group of six small to medium sized alterations around the summit of Co. Bravos Negros (max. extension 200 x 1000 m).
10. Center near UTM 466/7066. A small alterations east of Qda. El Hueso (max. extension 100 x 500 m).
11. Center near UTM 457/7051. A medium sized alteration southeast of Co. Valiente (max. extension 500 x 1000 m).
12. Center near UTM 457/7049. A small alteration northeast Agua Amarga (max. extension 500 x 1000 m).

13. Center near UTM 465/7049. A small alteration at the northeastern end of the Qda. Colorado (max. extension 300 x 1000 m).
14. Center near UTM 468/7050. A small alteration west of Co. Bravo Alto (max. extension 300 x 300 m).
15. Center near UTM 469/7048. Group of two small alterations southwest of Co. Bravo Alto (max. extension 300 x 300 m).
16. Center near UTM 465/7048. Two large alterations around Co. Indagua (test site I, max. extension 2000 x 2500 m).
17. Center near UTM 458/7042. A medium sized alteration southwest of Co. Tamberia (max. extension 1000 x 1300 m).
18. Center near UTM 452/7040. A medium sized alteration in the northern Qda. Agua Amarga (max. extension 1000 x 2500 m).
19. Center near UTM 472/7039. Group of four small to medium sized alterations north of Co. Vicuñita (max. extension 500 x 1000 m).
20. Center near UTM 473/7036. A large alteration north of Can Can, called Ciopa Norte (test site II, max. extension 1000 x 1200 m).
21. Center near UTM 473/7035. The medium sized alteration of Can Can (test site II, max. extension 1000 x 1000 m).
22. Center near UTM 472/7035. A medium sized alteration west of Can Can, called Margarita (test site II, max. extension 1000 x 1000 m).
23. Center near UTM 474/7034. A large alteration southeast of Can Can, called La Ciopa (Ladera-Farellon) (test site II, max. extension 2000 x 1500 m).
24. Center near UTM 475/7031. A large alteration southeast of La Ciopa, called Paloma (max. extension 1000 x 1200 m).
25. Center near UTM 475/7031. A large alteration southwest of La Ciopa (Ladera-Farellon), called Paloma (max. extension 1500 x 2500 m).
26. Center near UTM 475/7035. A medium alteration northwest Can Can, called Pompeya (max. extension 800 x 1000 m).

5.4 The ASTER approach

In late 1999 the **A**dvanced **S**paceborne **T**hermal **E**mission and Reflection **R**adiometer (ASTER) was launched onboard the new *Terra* satellite (NASA, 2004). With its new geometric resolution (Fig. 21) and up-to-date images it was possible to verify if some of the detected alteration sites (see above) were further explored or even under mineral exploration/mining. It is interesting to see that especially at the La Coipa test site an intense mining activity took place since the mid 1990'ties and is still under process until today. It underlines that the multispectral remotely detected mineral alterations and their 'spectral surface fingerprints' relate strongly to economically exploitable mineral resources. Figure 22 reveals the details of the new mine La Coipa with its dumps and facilities (the IR-scene was shot in January 2003). Therefore we strongly recommend the further use of new multispectral satellite data (like *Ikonos* or *Quickbird*) to explore the mineral and geological potential of remote areas.

Characteristic	VNIR	SWIR	TIR
Spectral Range	Band 1: 0.52 - 0.60 µm Nadir looking	Band 4: 1.600 - 1.700 µm	Band 10: 8.125 - 8.475 µm
	Band 2: 0.63 - 0.69 µm Nadir looking	Band 5: 2.145 - 2.185 µm	Band 11: 8.475 - 8.825 µm
	Band 3: 0.76 - 0.86 µm Nadir looking	Band 6: 2.185 - 2.225 µm	Band 12: 8.925 - 9.275 µm
	Band 3: 0.76 - 0.86 µm Backward looking	Band 7: 2.235 - 2.285 µm	Band 13: 10.25 - 10.95 µm
		Band 8: 2.295 - 2.365 µm	Band 14: 10.95 - 11.65 µm
		Band 9: 2.360 - 2.430 µm	
Ground Resolution	15 m	30m	90m
Data Rate (Mbits/sec)	62	23	4.2
Cross-track Pointing (deg.)	±24	±8.55	±8.55
Cross-track Pointing (km)	±318	±116	±116
Swath Width (km)	60	60	60
Detector Type	Si	PtSi-Si	HgCdTe
Quantization (bits)	8	8	12
System Response Function	VNIR Chart VNIR Data	SWIR Chart SWIR Data	TIR Chart TIR Data

Fig. 21: Technical specification of the ASTER remote sensing sensor (modified after NASA, 2004).

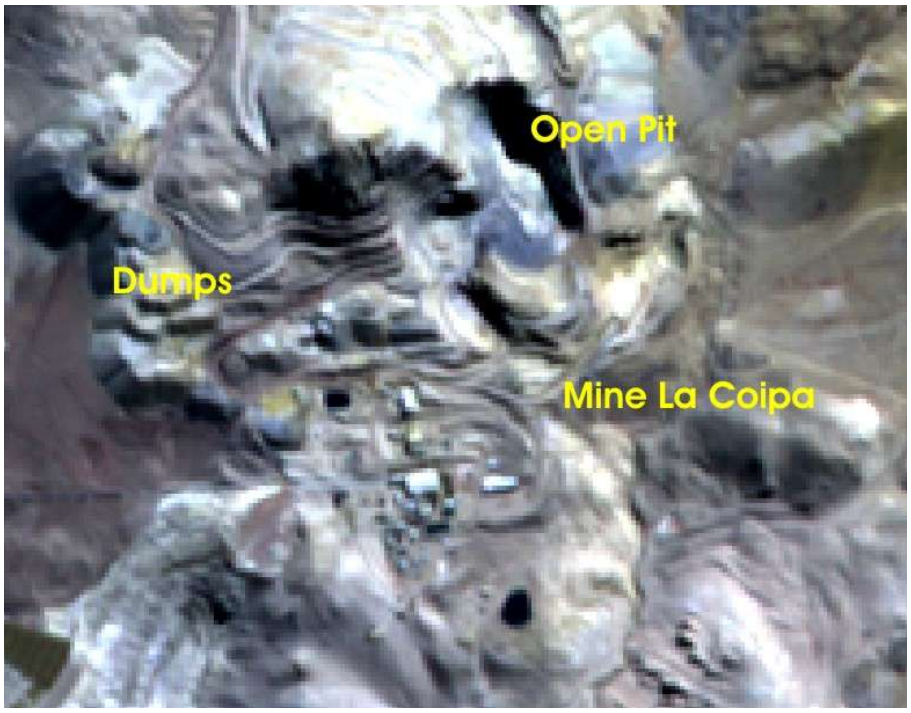

Fig. 22: Established Au-Ag-Mine La Coipa in January 2003 (run by Placer Dome Inc., Canada; for more details see http://www.placerdome.com/operations/lacoipa/lacoipa.html) as seen by the ASTER Satellite (15m/Pixel). In this IR-image the mineral alterations are general characterized by a bright albedo.

6 Summary and conclusions

The combination of field observations with remotely sensed data for the detection and extrapolation of hydrothermally altered rocks has often been applied in mineral exploration. (ROWAN & KAHLE, 1982; PODWYSOCKI et al., 1983; KAUFMANN, 1989; PRINZ & BISCHOFF, 1995) but the quality of obtained results differs strongly depending on the used data (type of sensor) and the various geologic field conditions. Concentrating on the selected test sites within the Maricunga Belt we can state that the described remote sensing methods (basically OIF) led to a good reliability of multispectral CC's for the detection of spectral anomalies related to concentrations of indicative mineral suites if the statistical decision criteria and the laboratory spectra are considered. These criteria have also been found a useful tool to check the described multispectral mapping approach with some supervised lithological classification of mineral-sensitive ratios, calculated principal components or hybrid CC's for sites of known prospects like La Coipa or Indagua. Especially the discrimination of carbonatic lithological units from OH- or Fe-bearing rocks is supported by this methodology. All CC's successfully distinguished most types of altered rocks (acid-sulfate type) from unaltered volcanic or sedimentary rocks. Furthermore some previously unrecognized areas of hydrothermally altered rocks were detected southeast of Co. Dragon and north of Co. Colorado (Indagua test site) or near Paloma (La Coipa test site) as future prospects. Vice versa a detailed mapping of zones of different alteration intensities within some larger, coherent alteration areas is often hampered by the high overall brightness/albedo of silicified surfaces, additional spectral masking effects caused by Fe-rich hematitic crusts (desert varnish) and the insufficient spectral/spatial resolution of the TM scanner.

Although field studies have shown that most of the alterations are controlled by regional tectonic fracture systems (mainly transpressional induced, secondary NE-SW orientated faults) the relationship of those regional patterns to a larger, superior structural province (mainly NW-SE striking Indagua Fault, Bally Willis Fault, Agua Armaga Fault etc.) can only be deduced by analysing the extension of alteration zones in satellite data. This analysis can also be used in conjunction with field studies for interfering spatial and temporal relationships if the applied sensor shows a sufficient geometric resolution. Using the 30 m/pixel resolution of the TM scanner it became obvious that the smaller NE-SW orientated zones of stronger alterations (which were mapped during the field campaigns) are merely to detect due to their limited extension within the vaste areas of moderately altered rocks. The additional analysis of ASTER-data with its higher spatial resolution (but limited radiance sensability at 15m/pixel) combined with DGM-data supports the observation that the overall orientation of the hydrothermally altered surfaces seems to be influenced by the major tectonical structures of the Maricunga Belt (like the N-S striking faults of the West Fissure System).

Summarizing all of the above, we can state that the described image processing techniques provide the mineral explorationist with greatly expanded reconnaissance and detailed pre-field mapping knowledge for the Maricunga Belt. The data is very reliable for rapid hydrothermal alteration mapping, for finding the most prospective outcrop within the large, sometimes only hard to access areas of the Chilean Andes, and for drawing attention to subtle, often unsuspected prospects. For more specific applications, such as tracing the further extension of known mineralizations down to a bigger scale, the multispectral analyses should be based on scanner data wich allows a higher spectral and spatial resolution.

Acknowledgements
The authors are grateful to the staff of the remote sensing group of the BGR in Hannover for their help during the spectral analysis. Thanks are due to W. Griem, H. Sylvester, S. Sindern, B. Hellebrandt, N. Väth, A. Abels, H. Musial and all the others who contributed some of their field results during the mapping campaigns of the GPI in Chile. The University of Atacama/Copiapo, especially R. Cespedes Valenzuela is gratefully acknowledged for their cooperation and support. Homestake S.A./Chile and Manto de Oro/La Coipa are thanked for their cooperation and logistic efforts. The staff of the Dept. for Remote Sensing/GIS of the GPI in Muenster are thanked for their technical help during the preparation of the script. Furthermore the authors would like to thank the DFG for their financial support.

Literature

ABELS, A. (1995): Geologie der Sierra Sarabia in der Region Potrerillos (Nordchile, III. Region). - Diploma-Thesis, Geol. Inst., Univ. Münster, 116 p.; Münster.

ABELS, A. & BISCHOFF, L. (1996): Eocene Incaic orogenic phase in the Chilean Precordillera between 25°30'S-27°30'S related with large block-rotations? - 15. Geowiss. Lateinam. Kolloq. Hamburg, Terra Nostra, **8:** p. 13; Hamburg.

AGUILAR, A. G. (1984): Geologia de los Quadrangulos Cerro Vicunita y Salar de Maricunga, III. Region de Atacama, Chile. - Diploma Thesis, Geol. Inst., Univ. Antofagasta; Antofagasta.

CHAVEZ, P. S., BERLIN, G. L. & SOWERS, L. B. (1982): Statistical methods for selecting Landsat MSS ratios. - Jour. Appl. Photogr. Eng., **8:** p. 30-32.; London.

CORNEJO, P., MPODOZIS, C., RAMIREZ, C. F. & TOMLINSON, A. J. (1993): Estudio Geologico de la region de Potrerillos y El Salvador (26° - 27° Lat. S.). - Serv. Nat. Geol. Min., p. 258; Santiago (CODELCO).

CROSS, T. A. & PILGER, R. H. (1982): Controls of subduction geometry, location of magmatic arcs, tectonics of arc and back-arc regions. - Geol. Soc. Am. Bull., **93:** p. 545-562; Boulder.

DAVIDSON, J. & MPODOZIS, C. (1991): Regional geologic setting of epithermal gold deposits, Chile. - Econ. Geol., **86:** p. 1174-1186; Lancaster.

DONKER, N. H. W. & MULDER, N. J. (1976): Analysis of MSS digital imagery with the aid of principal component transformation. - XIII ISP Congr.; Helsinki..

DRURY, S. A. (1987): Image interpretation in Geology. - 243 p.; London.

GILLESPIE, A. R. (1980): Digital techniques of image enhancement. - In: Siegal, B. S. & GILLESPIE, A. R. (eds.): Remote sensing in Geology. - p.136-220; New York.

GRIEM, W. (1994): Strukturgeologisch-petrographische und geochemische an Gangesteinen und deren magmatischen Äquivalenten im Andensegment bei 27° südlicher Breite (Region Atacama, Nordchile). - Münster. Forsch. Geol. Paläontol., **75:** 139 p.; Münster.

GRUNICKE, J. M. (1990): Methodische Untersuchungen zur digitalen Bildverarbeitung von Fernerkundungsdaten: Lithologie und Tektonik der zentralen Lechtaler Alpen, Tirol, Österreich. - Berl. Geow. Abhdl., **121:** 115p; Berlin.

HELLEBRANDT, B. (1993): Geologie und Petrologie der Subvulkanite und Effusiva im südlichen Au-, Ag-Lagerstättenbezirk von La Coipa (Region Atacama, Nordchile). - Diploma-Thesis, Geol. Inst., Univ. Münster, 105 p.; Münster.

KAUFMANN, H. (1989): Image processing strategies for mineral exploration in arid areas by use of TM-data.- ESA-Rep., **SP1102:** p. 111-125; Frascati (ESA).

KLEY, J., REUTTER, K. J. & SCHEUBER, E. (1991): Die zentralen Anden. Geologische Strukturen eines aktiven Kontinentalrandes. - Geol. Rundschau, **43** (3): p. 135-142; Stuttgart.

LOUGHLIN, W.P. (1991): Principal component analysis for alteration mapping.- Photogr. Eng. & Rem. Sens., Vol. **57 (9):** p. 1163-1169; Denver.

MCBRIDE, S. L., CAELLES, J. C., CLARK, A. H. & FARRAR , E. (1976): Paleocoic radiometric age provinces in the Andean basement, Lat. 25° - 30°S. - Earth Plan. Sci. Let., **29:** p. 373-383; Amsterdam.

MOSCOSO, R., CUITINO, L., MAKSAEV, V. & KOEPPEN, R. (1992): El complejo Cerros Bravos: macro volcanologico para la alteracion y mineralizacion en la franja de Maricunga, Copiapo, Chile.- In: Seminario Taller: Procesos formadores de depositos epitermales de metales preciosos. - p. 53-54; Santiago.

MPODOZIS, C., CORNEJO, P., KAY, S. M. & TITTLER, A. (1995): La Franja de Maricunga: sintesis de la evolution del Frente Volcanico Oligoceno-Mioceno de la zona sur de los Andes Centrales. - Rev. Geol. Chile, **21 (2):** p. 273-313; Santiago.

NASA (2004): The characteristics of the new ASTER sensor as described under HTTP://EOSPSO.GSFC.NASA.GOV.

OLSON, S. F. (1989): The stratigraphic and structural setting of the Potrerillos Porphyry Copper district, northern Chile. - Rev. Geol. Chile, **16 (1):** p. 3-29; Santiago.

PERKIN-ELMER (1993): The Lambda-9 manual. - Perkin-Elmer, 45 p; Überlingen.

PINCHEIRA, M. J., THIELE, R. & FONTBOTE, L. (1990): tectonic depression along the southern segment of the Atacama Fault Zone, Chile. - In: Colloques et Seminaires, Symp. Int. Geodyn. Andine, p. 133-136; Grenoble.

PODWYSOCKI, M. H., SEGAL, D. B. & ABRAMS, M. J. (1983): Use of multispectral scanner images for assessment of hydrothermal alteration in the Marysvale, Utah, ming area. - Econ. Geol., **78:** p. 675-687; New Haven.

PRINZ, T. (1996): Multispectral remote sensing of the Gosses Bluff impact crater, central Australia (N.T.) by using Landsat-TM and ERS-1 data. - ISPRS Jour. Photogr. & Rem. Sens., **51:** p.137-149; Amsterdam (Elsevier).

PRINZ, T. & BISCHOFF, L. (1995): Lokalisierung hydrothermal veränderter Gesteine im Gebiet um Potrerillos (Nordchile) mit Hilfe multispektraler TM-Daten. - Münster. Forsch. Geol. Paläontol., **77:** p.105-120; Münster.

REUTTER, K. J. & SCHEUBER, E. (1988): Relation between tectonic and magmatism in the Andes of Northern Chile and adjacent areas between 21° and 25° S. - V. Congr. Geol. Chil., **I:** p. A345-A363; Santiago.

ROWAN, L. C. (1977): Discrimination of hydrothermally altered and unaltered rocks in visible and near infrared multispectral images.- Geophysics, **42:** p. 522-535; Tulsa.

ROWAN, L. C. & KAHLE, A. B. (1982): Evaluation of 0.046-2.36 æm scanner images of the east Tintic mining district, Utah, for mapping hydrothermally altered rocks.- Econ. Geol., **77:** p. 441-452; New Haven.

SABINS, F. F. (1986): Remote sensing: Principles and interpretation.- 426 p.; San Francisco (Freeman Press).

SCHEUBER, E. (1994): Tektonische Entwicklung des nordchilenischen Kontinentalrands: Der Einfluß von Plattenkonvergenz und Rheologie. - Geotek.t. Forsch. **81:** p. 1-131; Stuttgart.

SCHEUBER, E. & ANDRIESSEN, P. A. M. (1990): The kinematic and geodynamic significance of the Atacama Fault Zone, northern Chile. - Jour. Struc. Geol., **12 (2):** p. 243-257; Oxford (Pergamon).|

SCHEUBER, E., BOGDANOVIC, T., JENSEN, A. & REUTTER, K. J. (1994): Tectonic development of the north Chilean Andes in relation to plate convergenceand magmatism since the Jurassic. - In: REUTTER, K. J., SCHEUBER, E. & WIGGER, P. J. (eds.): Tectonics of the southern Central Andes. - p. 121-139; Stuttgart (Enke).

SINDERN, S. (1993): Geologie und hydrothermale Alterationen des nördlichen Au-, Ag-Lagerstättenbezirks von La Coipa (Nordchile, III. Region). - Diploma-Thesis, Geol. Inst., Univ. Münster, 106 p.; Münster.

SINDERN, S., HELLEBRANDT, B. & BISCHOFF, L. (1995): Hydrothermale Alteration und Goldvererzung im Bereich der Mine La Coipa, Atacama-Region, Nordchile. - Münster. Forsch. Geol. Paläontol., **77:** p.69-80; Münster.

SINDERN, S., HELLEBRANDT, B., BISCHOFF, L. & SYLVESTER, H. (1996): Miocene volcanism and tectonics in the La Coipa area, 27°S, Chile. - Zbl. Geol. Paläontol., **I (7/8):** p. 853-868; Stuttgart.

SKARMENTA, J.. (1985): Informe datacion No. 68/85. - SERNAGEOMIN, 9 p.; Santiago.

STOFFREGEN, G. T. (1992): genesis of acid-sulfate alteration and Au-Cu-Ag mineralizations at Summitville, Colorado. - Econ. Geol., **82:** p. 1575-1591; Lancaster.

SUAREZ, M., BELL, C. M. & HUTTER, T. (1994): Lower Triassic lacustrine sediments in La Coipa area, Atacama, Chile. - Jour. South Am. Earth Sci., **8 (1):** p. 9-15; New York.|

SYLVESTER, H. & PALACIOS, C. (1992): Transpressional structures in the Andes between the Atacama Fault Zone and the West Fissure System at 27° S, III. Region, Chile. - Zbl. Geol. Paläontol., **I (6):** p. 1645-1658; Stuttgart.

VÄTH, N. (1995): Geologie des Indagua Distriktes in der Domeyko-Kordillere (Region Atacama, Nordchile). - Diploma-Thesis, Geol. Inst., Univ. Münster, 140 p.; Münster.

VILA, T. & SILLITOE, R. (1991): Gold-rich Porphyry systems in the Maricunga Belt, Northern Chile. - Econ Geol., **86:** p. 1238-1260; Lancaster.